Design and Fabrication of Diffractive Optical Elements

Diffraction by opaque screens

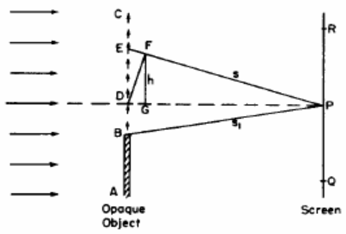

Fig. 30–7. A distant light source casts a shadow of an opaque object on a screen.

Fig. 30–9. The intensity near the edge of a shadow. The geometrical shadow edge is at x_0.

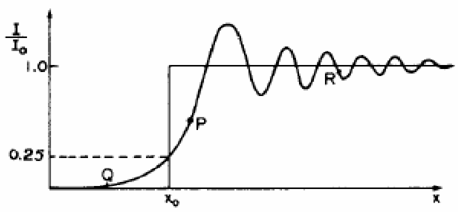

Function principle of DEs

Resulting Output Wave

$E(x', y', z_0+z)$

DE with Transmission Function

$T(x, y)$

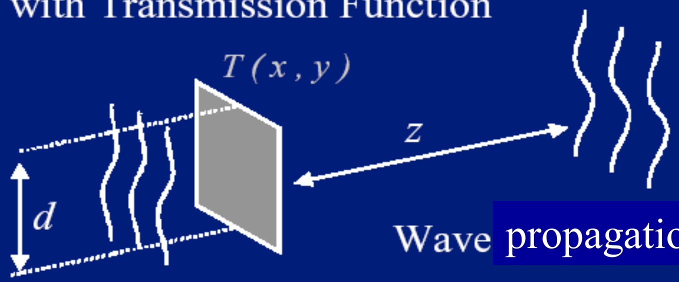

Wave propagation

Illumination Wave

$E(x, y, z_0)$

The illumination wave is modulated by the diffractive Element.

The modulated wave propergates through space and results in a certain desired signal wave.

From Refractive to diffractive Optics

$n = 1 - \delta + i\beta$

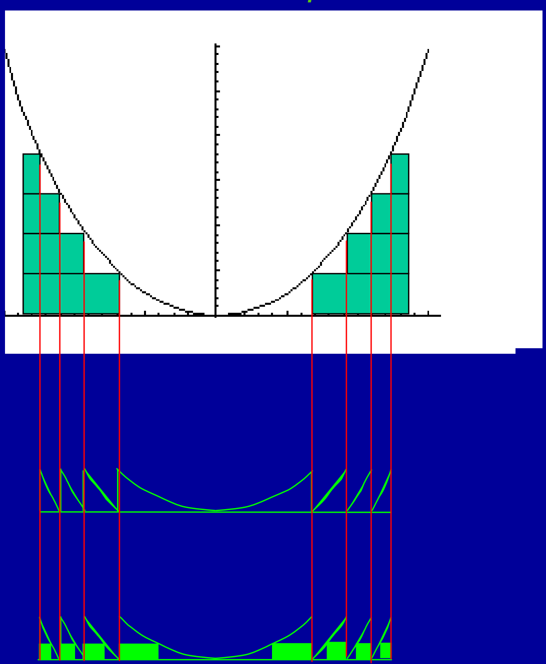

β: Imaginary part of complex refractive index;

λ: Incoming wavelength;

Refractive Profile

↓

Kinoform Profile:

minimize absorption and simplify fabrication.

μ: Abs. Coeffcient;

Δϕ: Phase shift;

t: Material Thickness;

$$\mu = \frac{4\pi}{\lambda}\beta$$

$$\Delta\phi = \delta(2\pi/\lambda)t = 2\pi$$

$$t(\Delta\phi = 2\pi) \rightarrow \lambda\delta^{-1}$$

$$r \approx (f\lambda)^{1/2}$$

Some Functions of Diffractive Elements

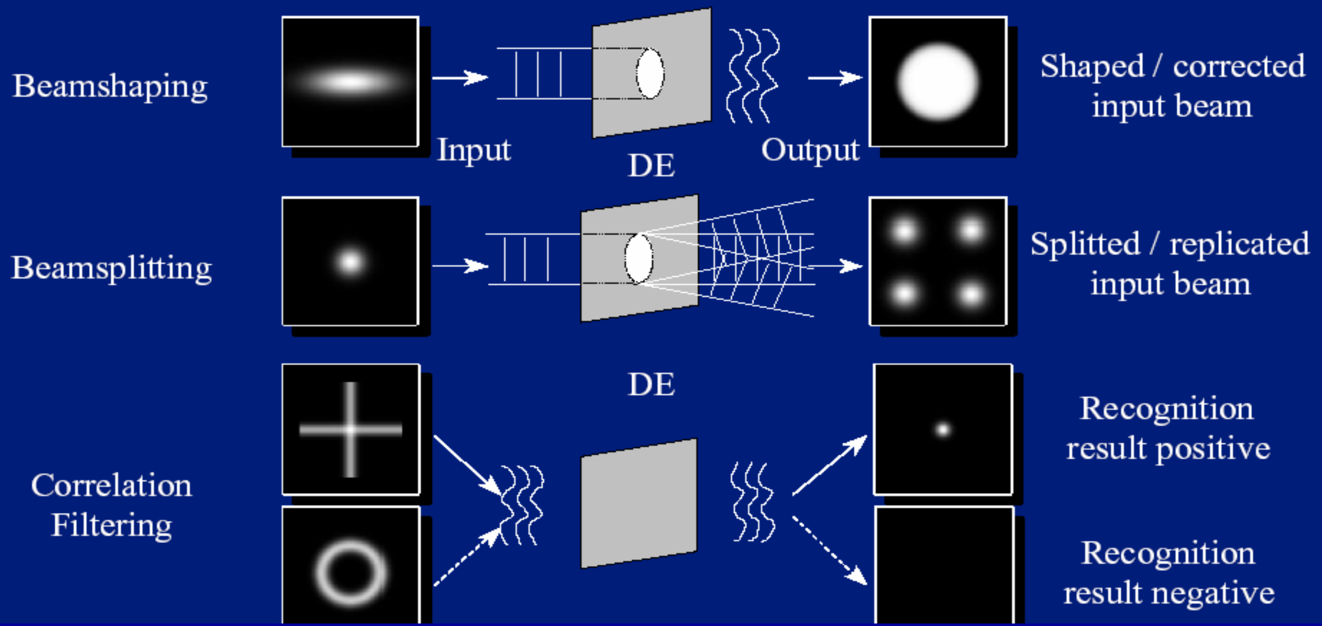

Realisation of Microstructures

Index-modulated structure

Surface-modulated structure

Example: liquid crystal displays

Example: fabrication by laser or e-beam lithography and etching

Fabrication Methods in Detail

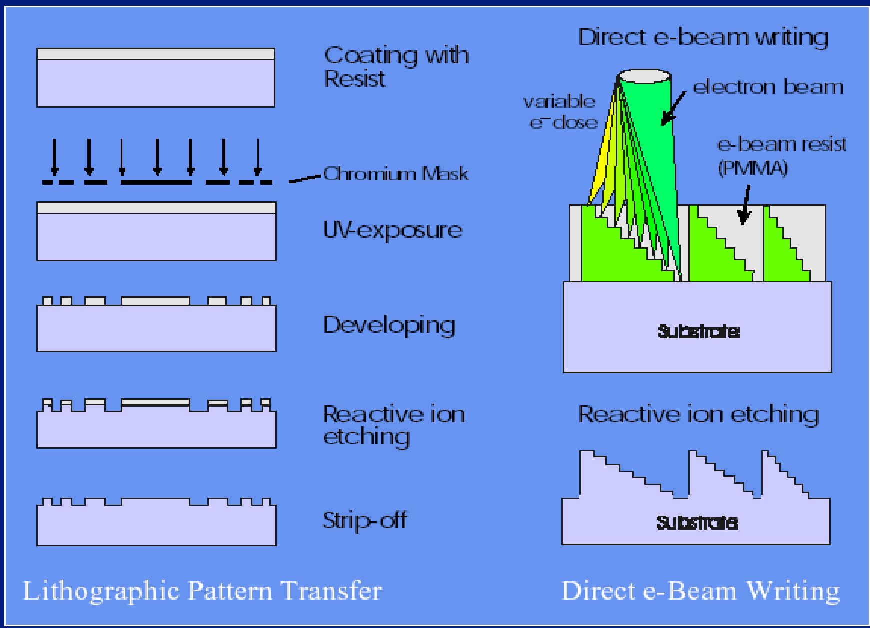

Binary DE

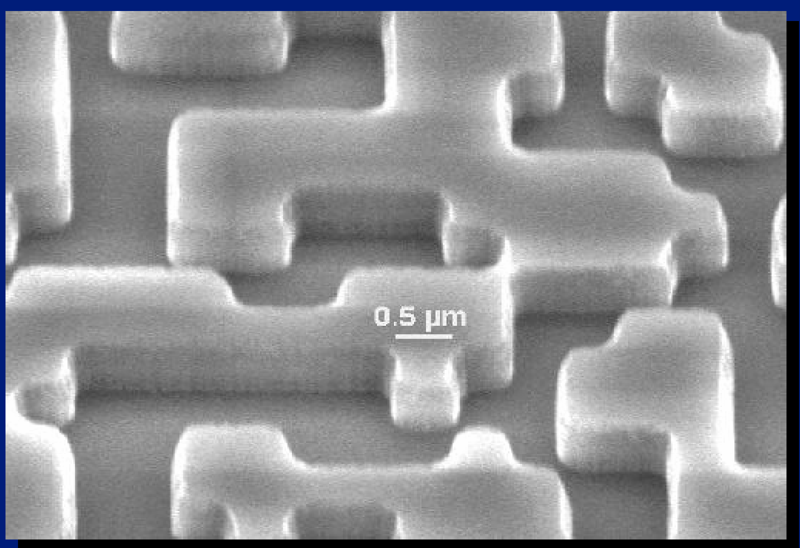

Binary structure of a beamsplitter

Smallest structures: 0.5 µm !

Continuous DE

Section of the designed 8-level structure of a beamsplitter

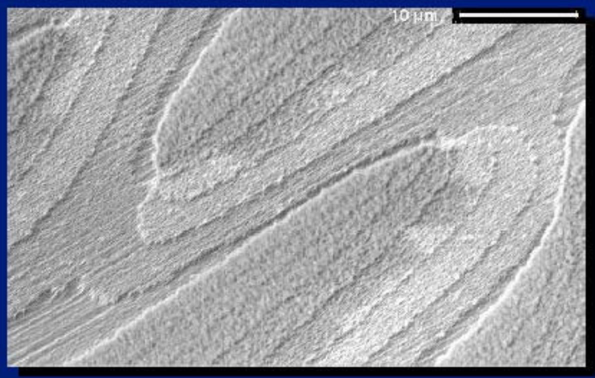

Section of the fabricated 8-level structure of a beamsplitter

Replication of DEs
Example: Injection Molding

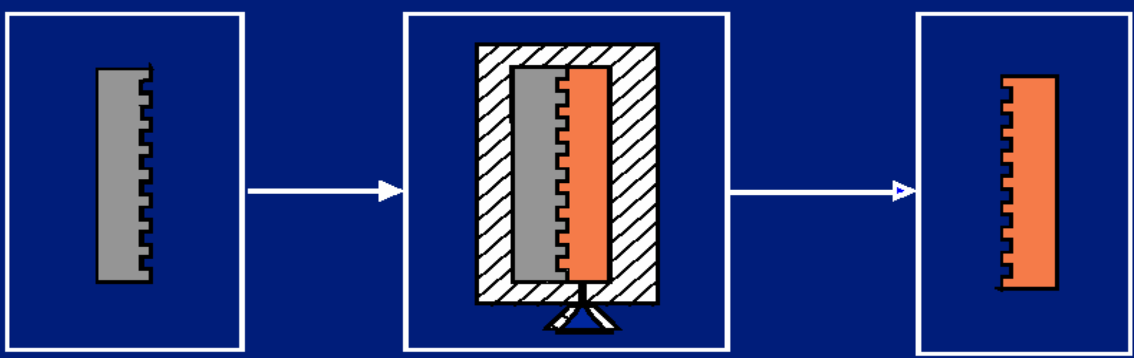

Microstructured Shim

Injection Molding Process

Microstructure in PMMA or Polycarbonate

Replication Methods

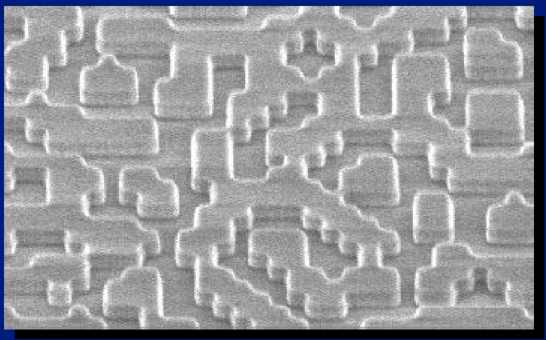

Section of a binary quartz-glass master

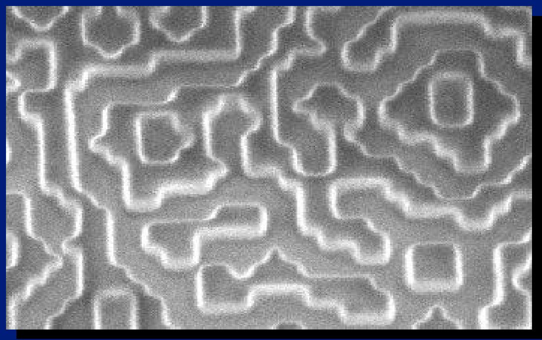

Section of replicated DE

Implementation Example: Beamshaping (technical analysis)

Square-line beamshaper:

- Output beam shape as specified
- Optical efficiency 86 % (theoretical)

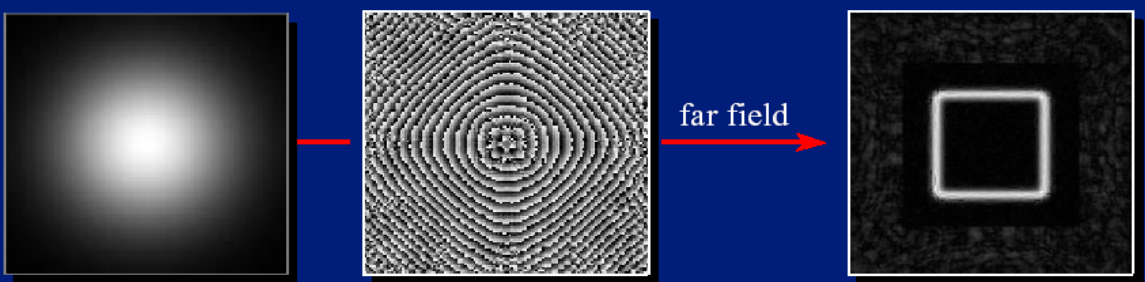

Illumination wave   16-level DE   Output wave

Implementation Example: Ringfocus (technical analysis)

Circle-line beamshaper:

- Output beam shape as specified
- Optical efficiency greater than 85 % (theoretical)

Implementation Example: Beamsplitter (fabricated)

1 to 40 ring beamsplitter:

- Deflection angle of each beam 15 °
- Optical efficiency 60 % ; uniformity of output beams

Implementation Example: Beamsplitter (technical analysis)

1 to 100 x 100 square beamsplitter:

- Optical efficiency 75% (theoretical)
- Uniformity of output beams

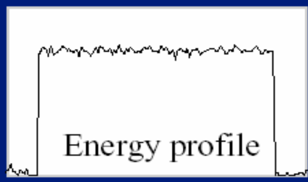

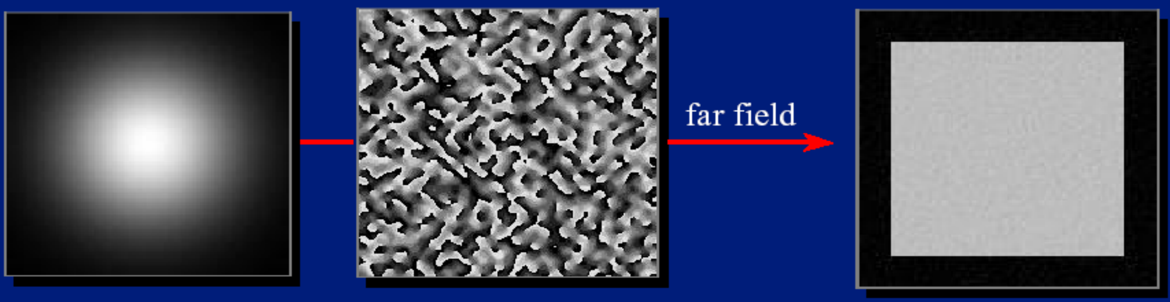

Illumination wave

8-level DE

Output wave:
100 x 100 light dots

Example: digital Hologram of Tutenchamun (fabricated)

Digital hologram:

- Output wave: image of Tutenchamun
- Minimum stray light

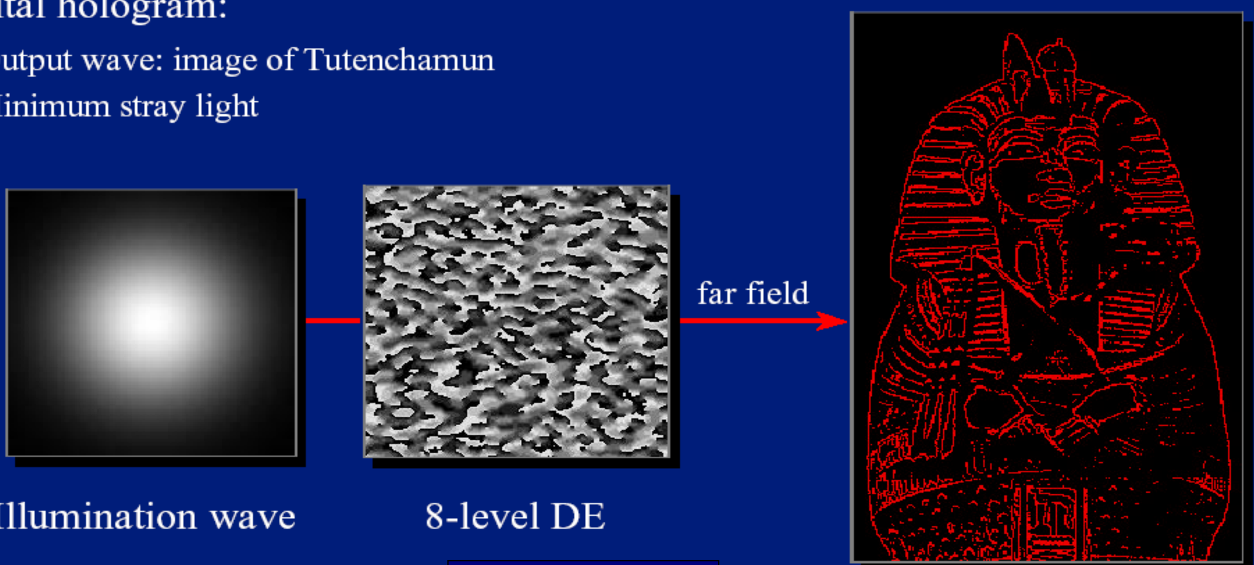

Illumination wave

8-level DE

DOE's design problem :

find the phase function, $\Phi_{DOE}(x)$, so that intensity distribution of the diffracted field, $I_g=|E_g|^2 \sim I_o$ (the desired intensity distribution) inside SW

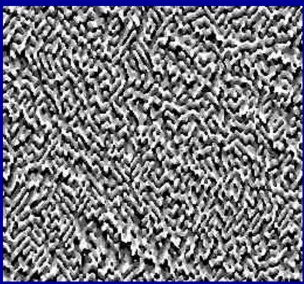

$\Phi_{DOE}(x)$

$$E_g(x;z) = P_z\{A_G(x)\exp[i\Phi(x)]\}$$

Diffracted Field Window (DFW)

Signal Window (SW)

Io = |Ao|² - desired intensity distribution
Φo - phase distribution **freedom degree**

Design approaches:

- ray traycing
- iterative optimization techniques
- **phase retrieval iterative algorithms**

- **ERA**: Error Reduction Algorithm, Aoi = Ao; DFW = SW
- **AAA** : Adaptive Additive Algorithm, Aoi = λAo+(1- λ)Aot inside SW; DFW > SW
- **CEA** : Combined Error Adaptive algorithm

Io = |Ao|² - desired intensity distribution
Φo - phase distribution **freedom degree**

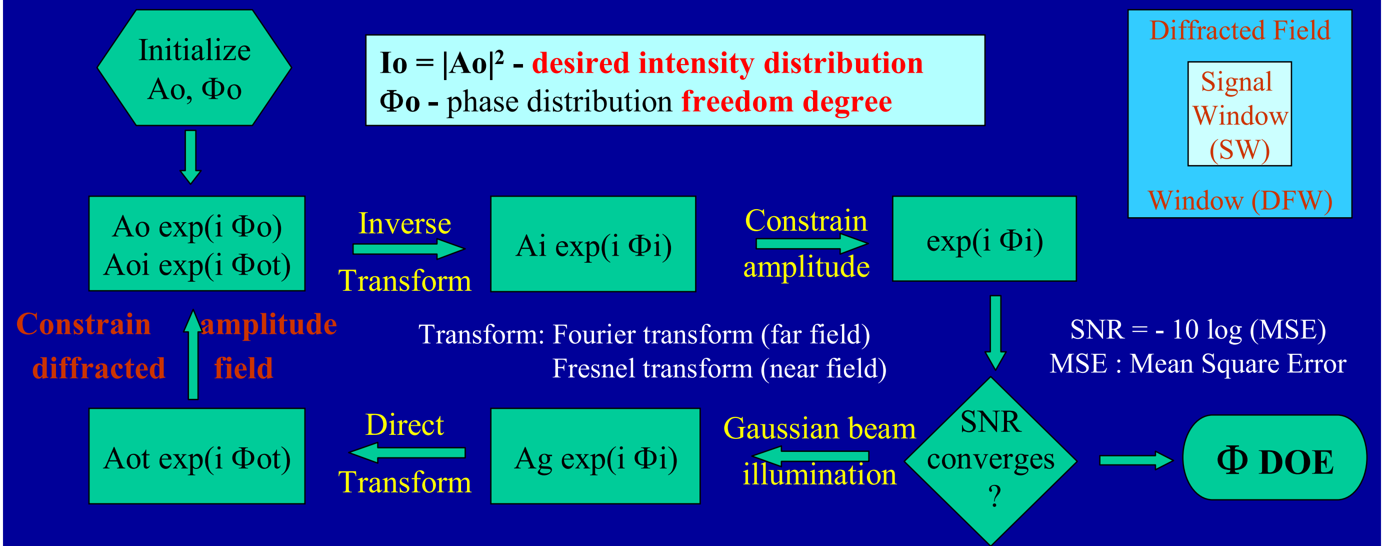

Computer simulation:
Phase-retrieval algorithms

Planar array of optical tweezers

Desired amplitude distribution in the signal window SW

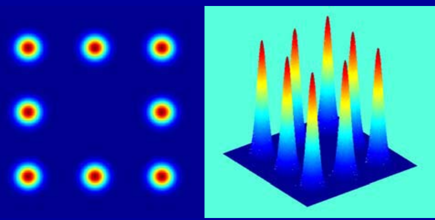

Phase DOE calculated with CEA

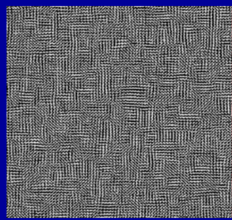

Size 1x1 mm
512x512 pixels
64 phase levels

Intensity distribution of the diffracted pattern obtained from DOE in the far field

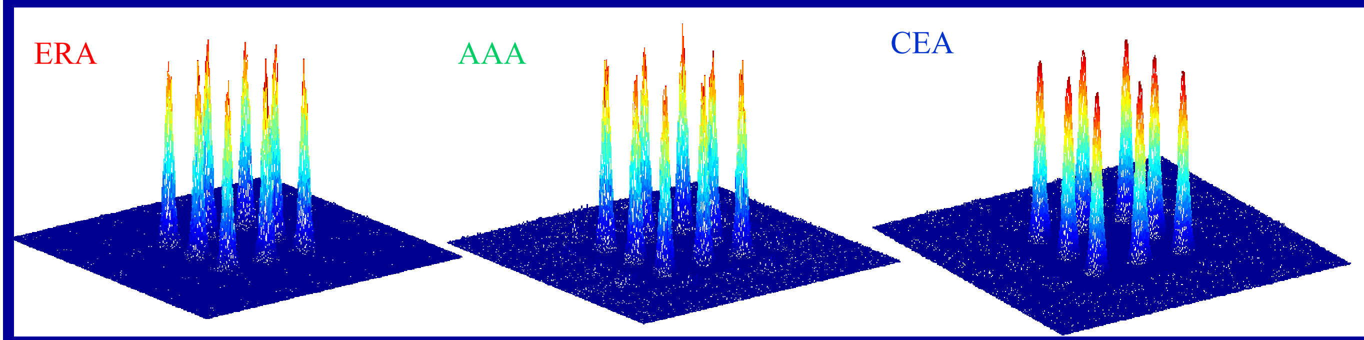

Computer simulations:
Phase-retrieval algorithms

Comparison of the iterative algorithms in terms of SNR

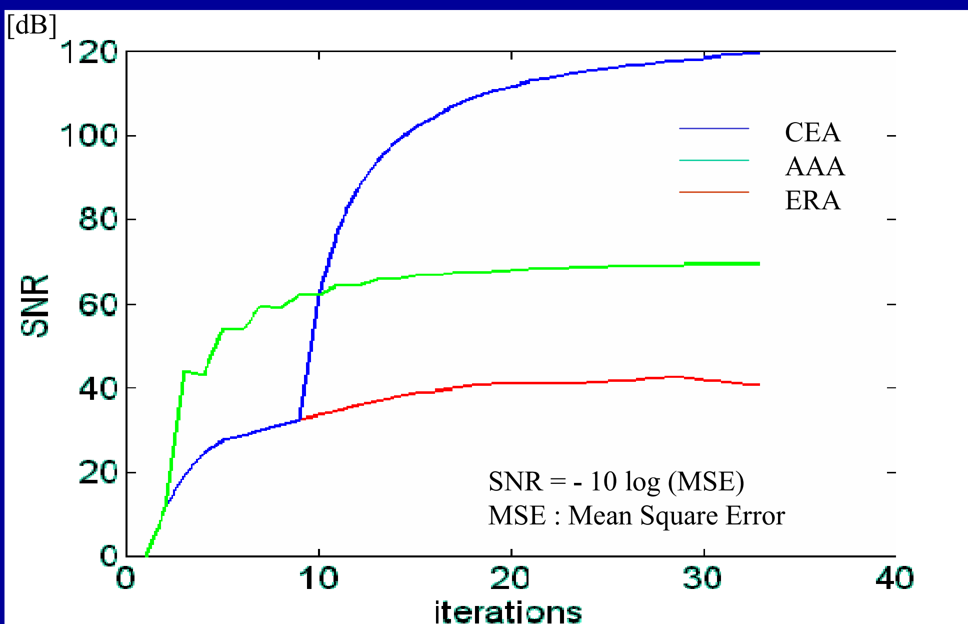

Computer simulation: CEA + Micro GA

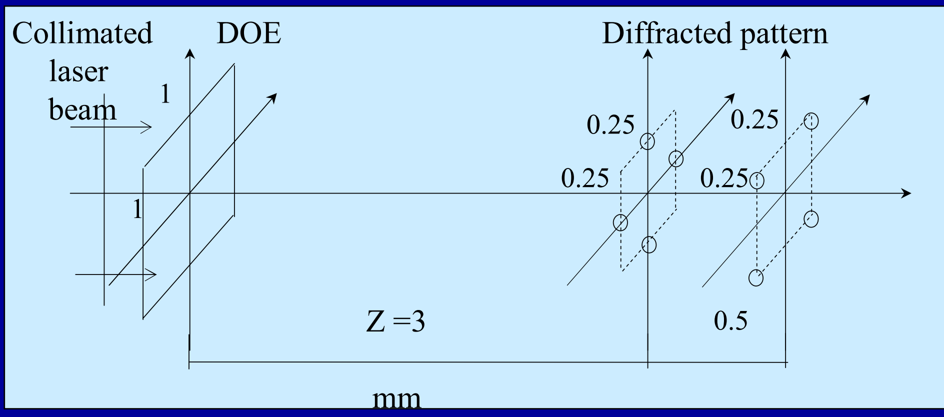

- CEA: calculate the phase functions corresponding to the two planar arrays (40 iterations)
- Micro GA: calculate the optimum phase function that creates the 3D array (40 iterations)

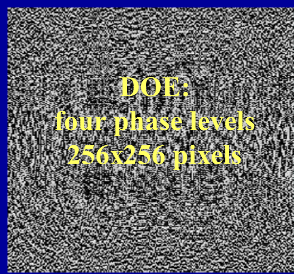

Computer simulation: CEA + Micro GA

Computed intensity distribution of the diffracted field

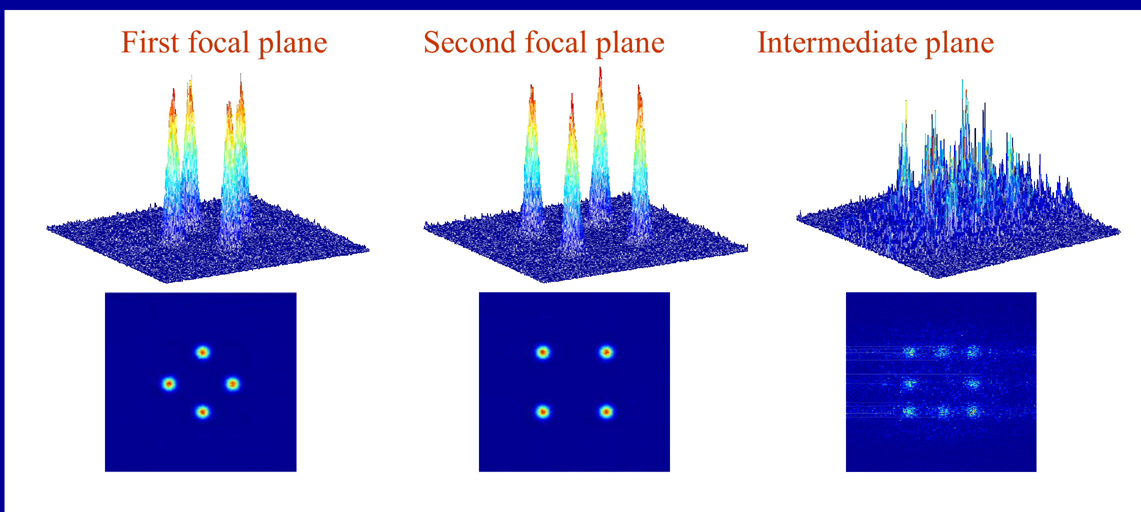

ICTP winter college 7-18 February 2005- Trieste

INFM-LILIT elettra

DOE's fabrication: flow chart

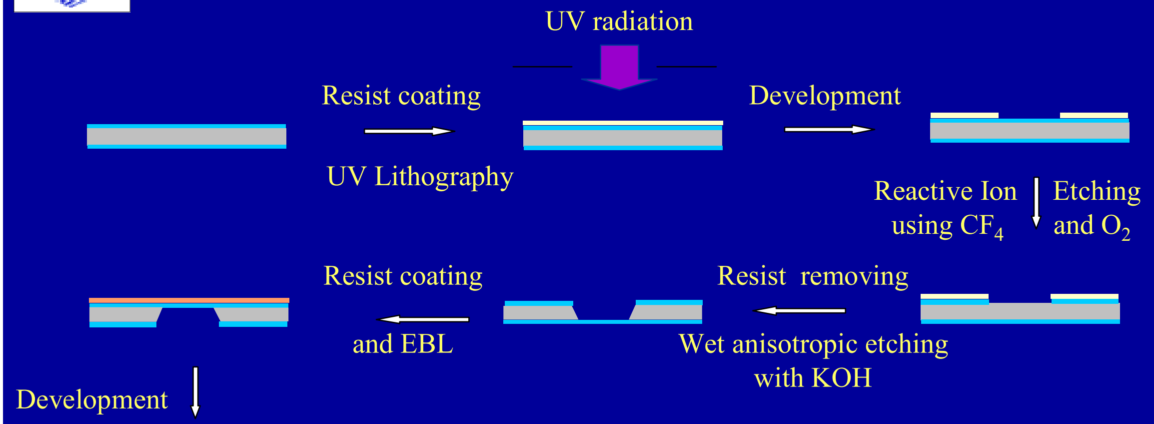

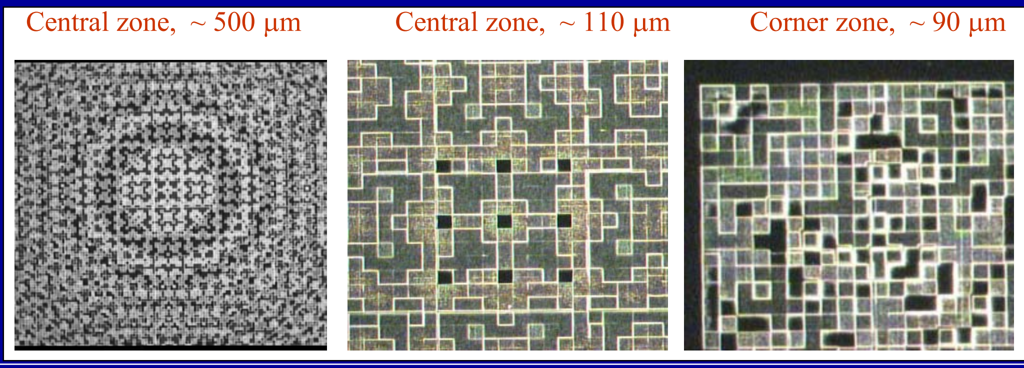

INFM-LILIT elettra

Experimental results: CEA + Micro GA

Detected intensity distribution of the diffracted field

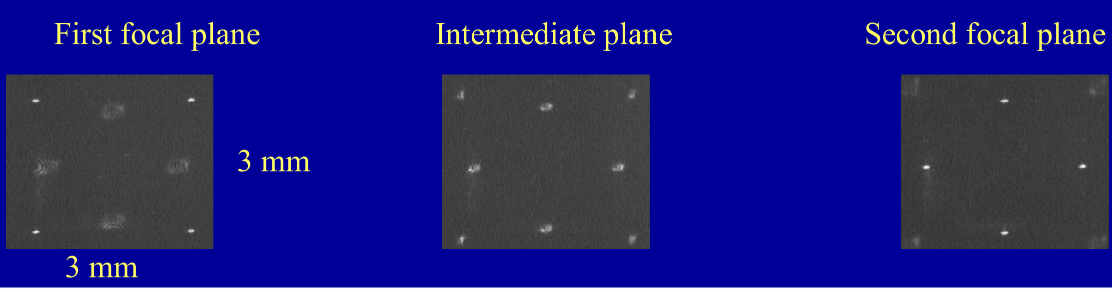

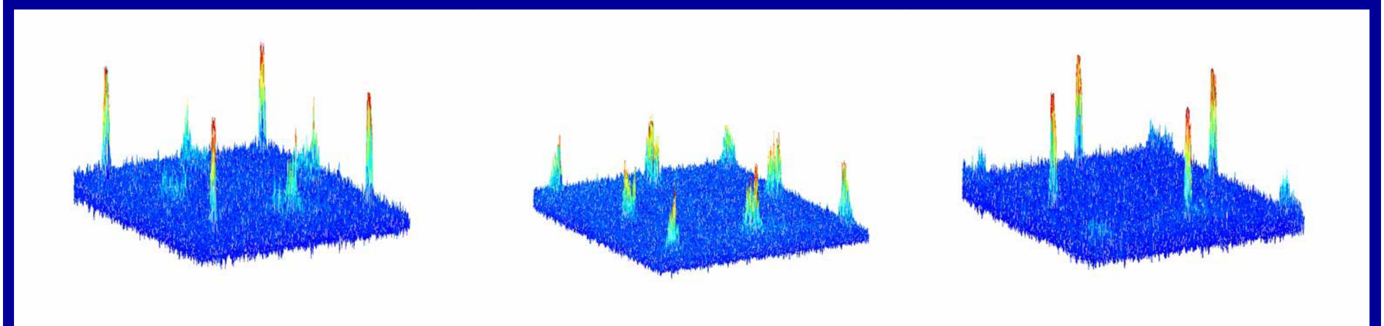

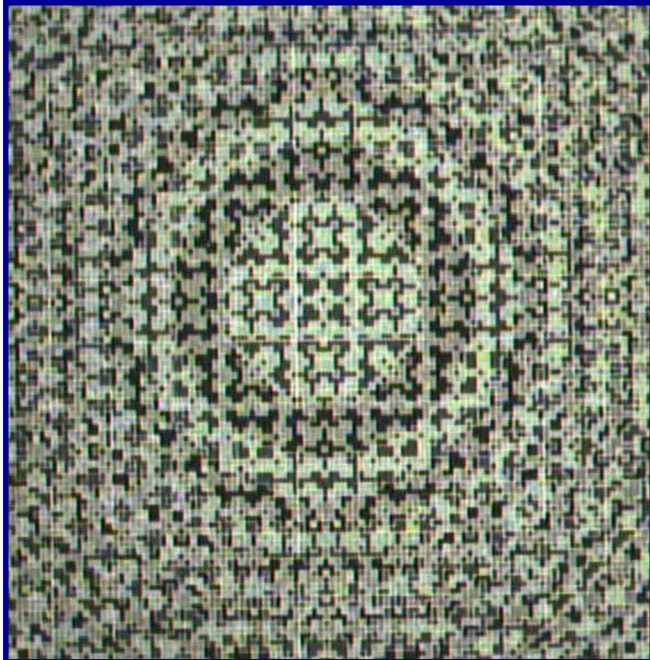

5x5 matrix for simultaneous Optical trapping

Diffractive nanopptics for DIC x-ray microscopy

1. Contrast in X-ray microscopy

Refractive index in X-ray region: **$n = 1 - \delta + i \cdot \beta$**

$\delta \rightarrow$ phase shift $\beta \rightarrow$ absorption

example: polyimide

photon energy [eV]	δ	β	δ / β
100	$2.3 \cdot 10^{-2}$	$4.9 \cdot 10^{-3}$	4.7
500	$1.1 \cdot 10^{-3}$	$3.2 \cdot 10^{-4}$	3.4
5000	$1.2 \cdot 10^{-5}$	$7.1 \cdot 10^{-8}$	170

$\rightarrow$ phase sensitive techniques superior to absorption contrast !

Motivation for microscopy techniques using phase information

Absorption contrast: $\sim E^{-3}$

Phase contrast: $\sim E^{-1}$

Use of phase shifting, real part of refractive index

- **orders of magnitude higher contrast**
- **tremendous reduction of dose applied to object**
- **additional transmission information on low side of absorption edges (XANES, XRF !)**

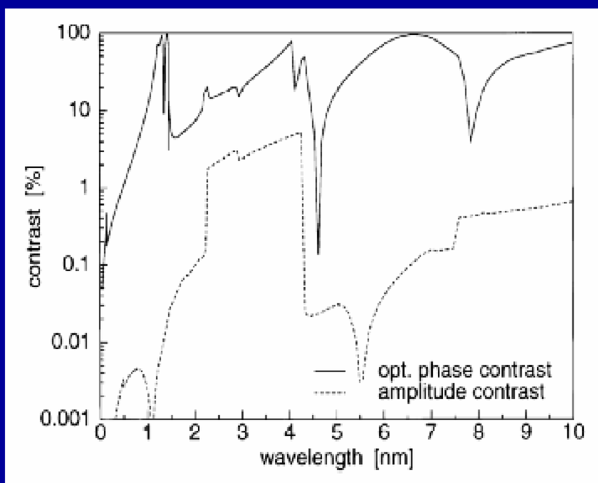

Amplitude and phase contrast for a model protein $C_{94}H_{139}N_{24}O_{31}$

General statements on DIC microscopy

Phase objects cannot be seen (difficult) when in focus with ordinary XRM (single ZP)

Phase objects retard or advance light that passes through them due to spatial variation in their refractive index and/or thickness

Needs for DIC microscopy

The image of DIC microscopes is formed from the interference of two mutually coherent waves with lateral displacements (shear) (of the order of the minimum size of the imaged structure and are phase-shifted relative to each other

Imaging characteristics

The intensity distribution in measured DIC images is given by a non linear function of the spatial gradient of a specimen's optical path length distribution along the direction of shear

Differential Interference Contrast DIC

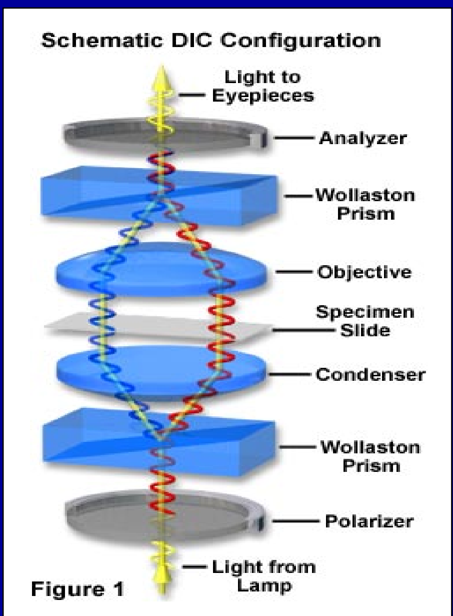

Visible light microscopy (Nomarsky set-up)

Shear of wave front division or distance of Airy disks in focal plane is smaller than optical resolution (*"differential"*)

DIC for X-ray microscopy with ZPs:

- Distance Δf of both ZPs smaller than depth of focus
- Displacement Δs smaller than resolution δ

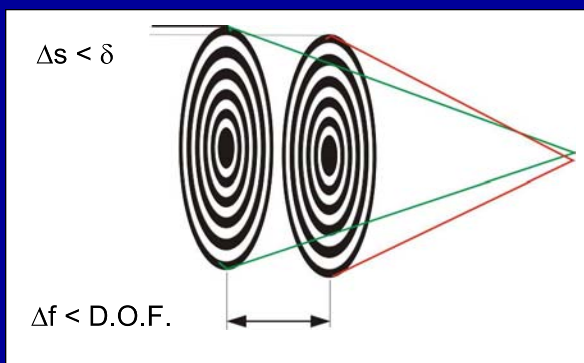

Differential Interference Contrast DIC

Working principle

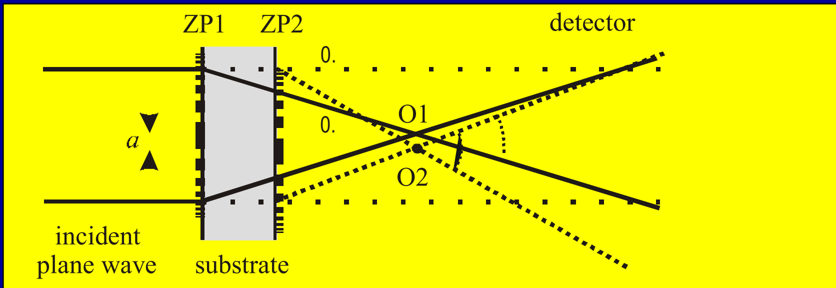

TXM set-up

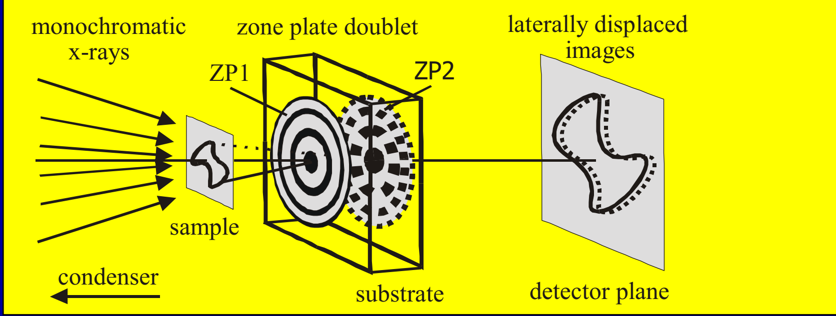

ZP doublet for X-ray microscopy in DIC mode

First ZP doublet generated by E. Di Fabrizio and S. Cabrini

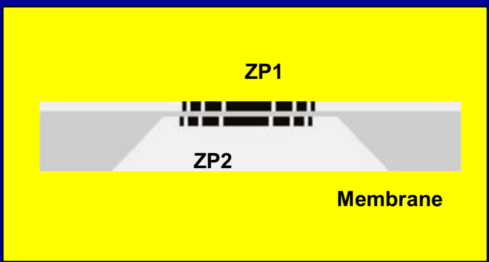

Technique: e-beam lithography and nanostructuring

Diameter:	**75 µm**
Outermost zone width:	**200 nm**
Focal length @ 4 keV:	**50 mm**
Efficiency:	**10 %**
Nominal displacement:	**100 nm**

Alignment markers definition

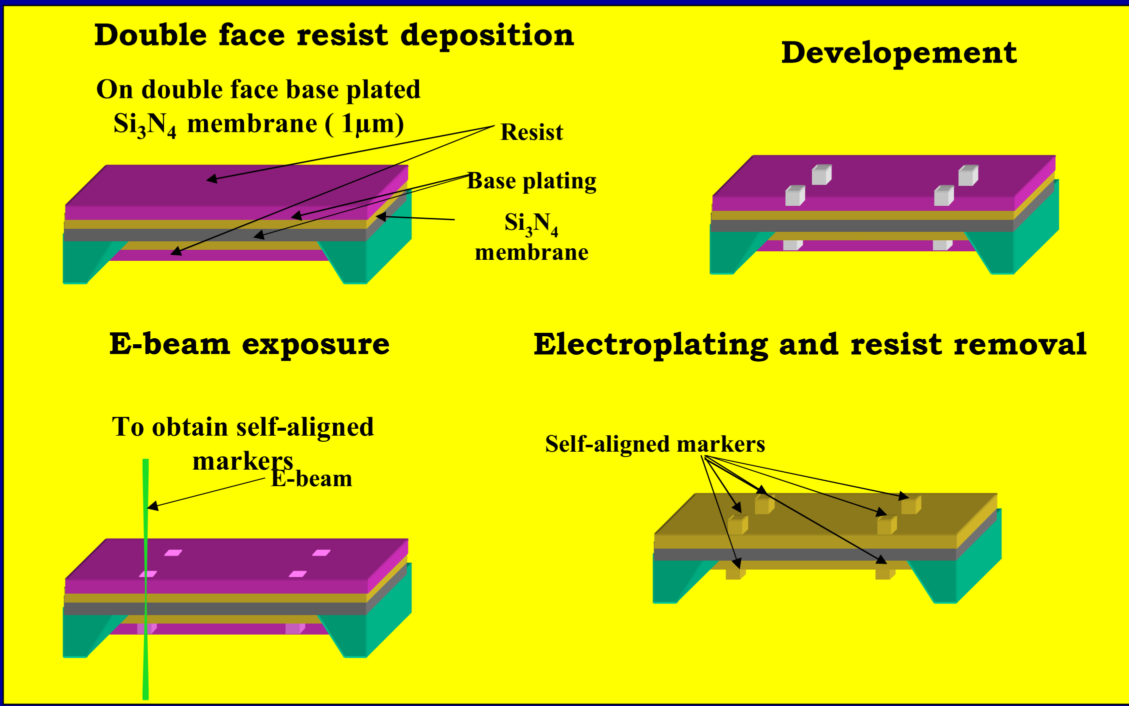

Double side ZP definition

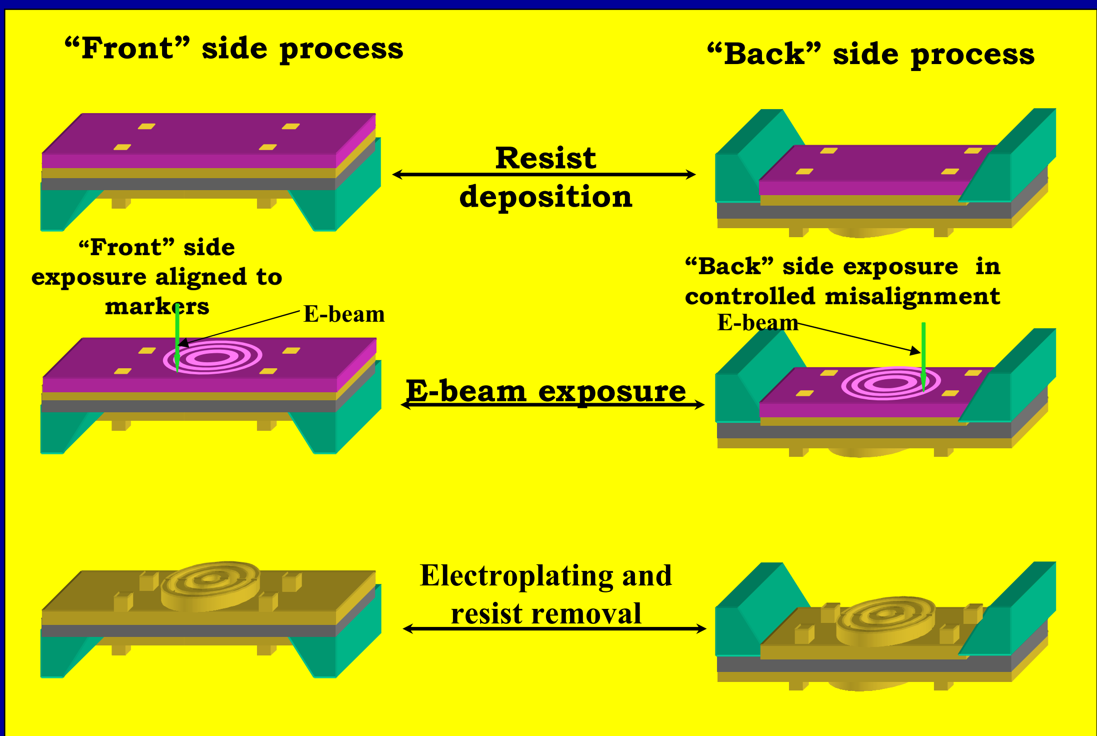

DIC objective (Back side view)
-May 2000-

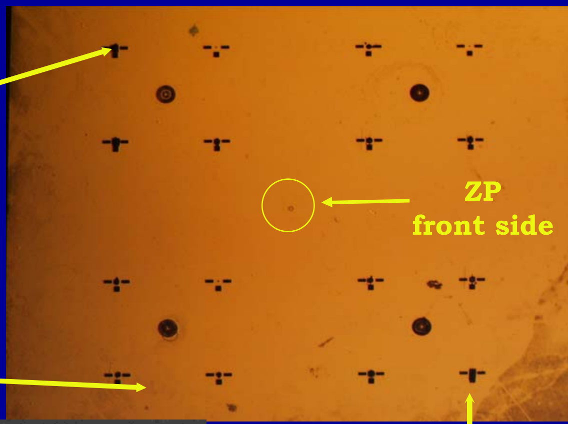

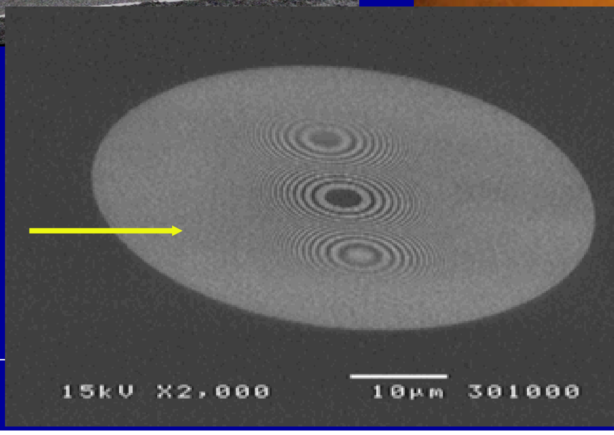

ZP front side

SiN membrane

Zone plate Objective

Alignment markers

Xray lithographic image of the ZP doublet

Efficiency of each zp=14%(first order)

Efficiency of zero order =35%

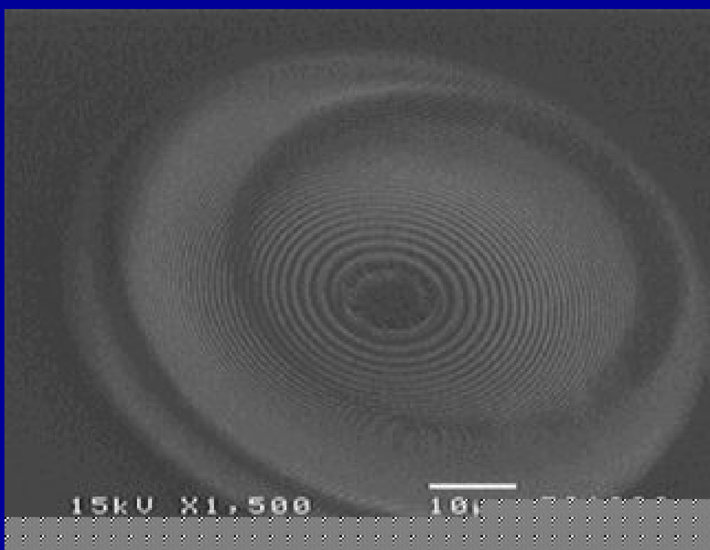

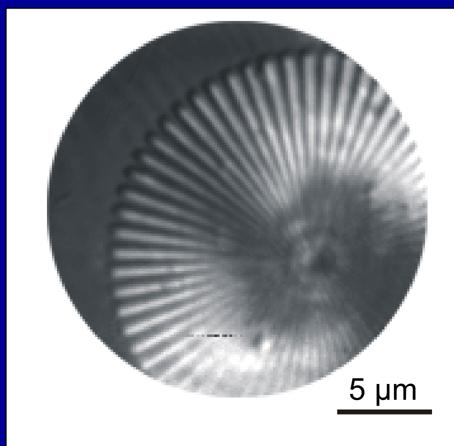

$\eta_{tot} = t_{ZP1}\eta_{ZP2} + t_{ZP2}\eta_{ZP1}$ =9.6%

Resolution test~ 160 nm

Potentiality of X-ray lithography for DIC fabrication for multi-keV energy

Expected fabrication parameters with Xray litho are:
- **Thickness**: no limitation (several tens of microns)
- **Resolution**: below 50 nm
- **Aspect ratio**: > 10 for sub 100 nm ZP resolution and > 15 above 200 nm ZP resolution
- **Controlled misalignment**: < 30 nm
- **Expected Xray energy**: above 10 keV

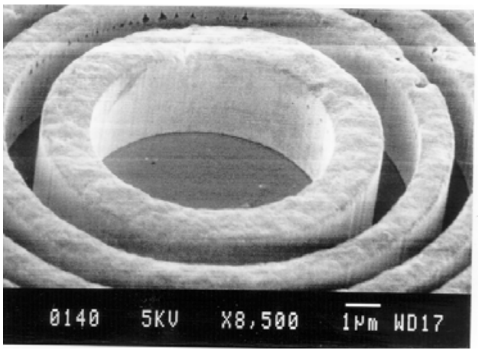

Depth of focus

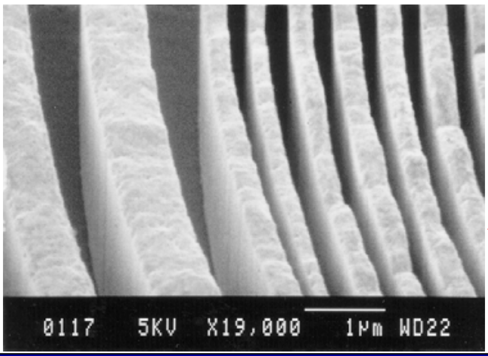

High resolution/ aspect ratio

Alignment accuracy

DIC X-ray microscopy with a full-field imaging microscope @ 4 keV

2 µm thick PMMA test structures with a transmission of 98.8 % @ 4 keV

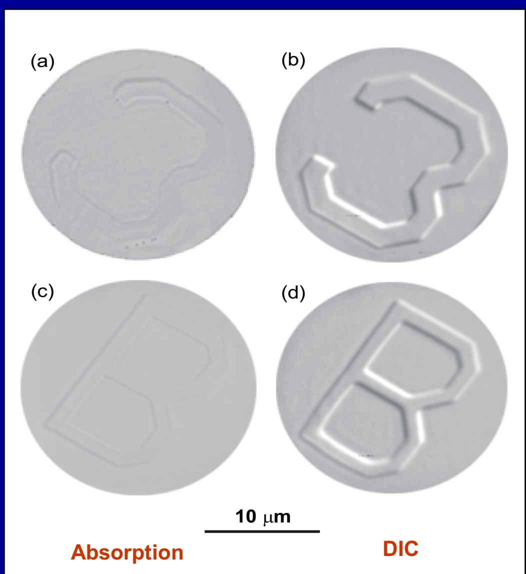

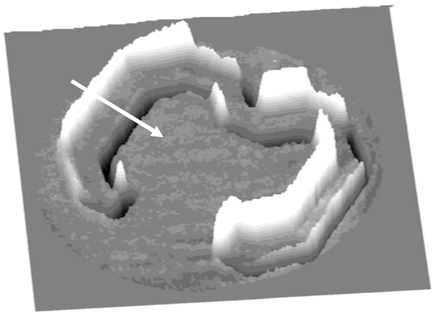

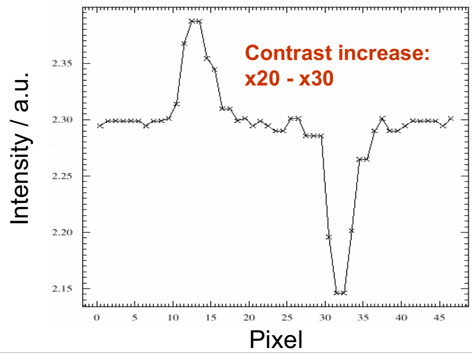

B. Kaulich, T. Wilhein, E. Di Fabrizio, S. Cabrini, F. Romanato, M. Altissimo, J. Susini (Nov 2000)

PMMA zone plate structure (250 nm)
2 micron thick:exposure time 10s

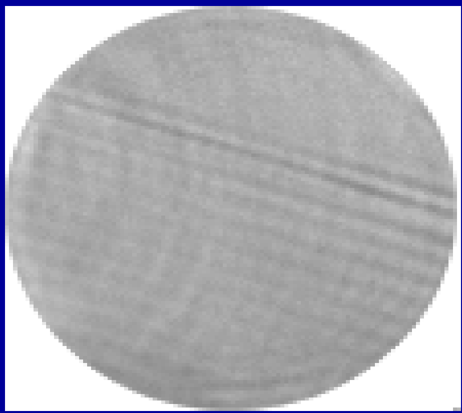

Bright field

5 µm

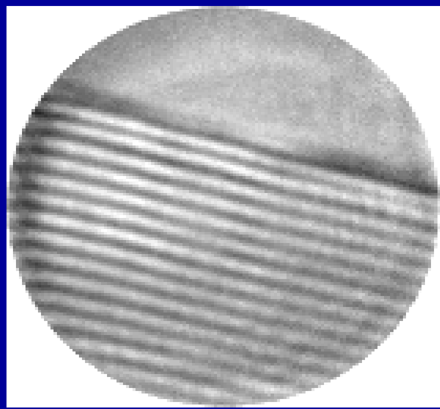

X-DIC transmission

General scheme of DOE shaping

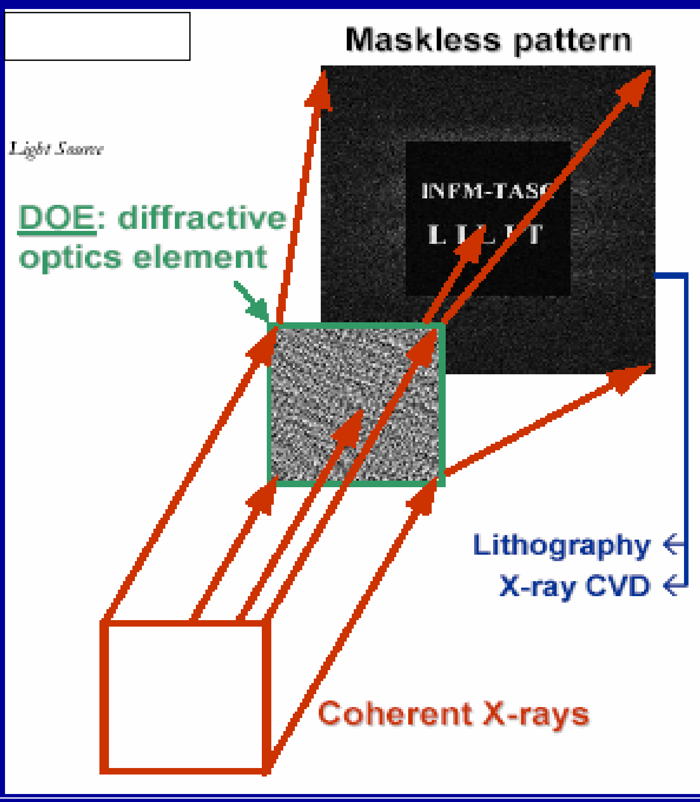

DOE's design

Numerical computation:

given a set of **input** data find the optimum **output** data which fit the requests

input data :

•Source space: wavelength, size, geometry, intensity distribution

•Image space: intensity or/and phase or/and polarization field distribution

•DOE: size, resolution, material

output data:

•DOE's phase or/and amplitude function

Diffractive optical element scheme

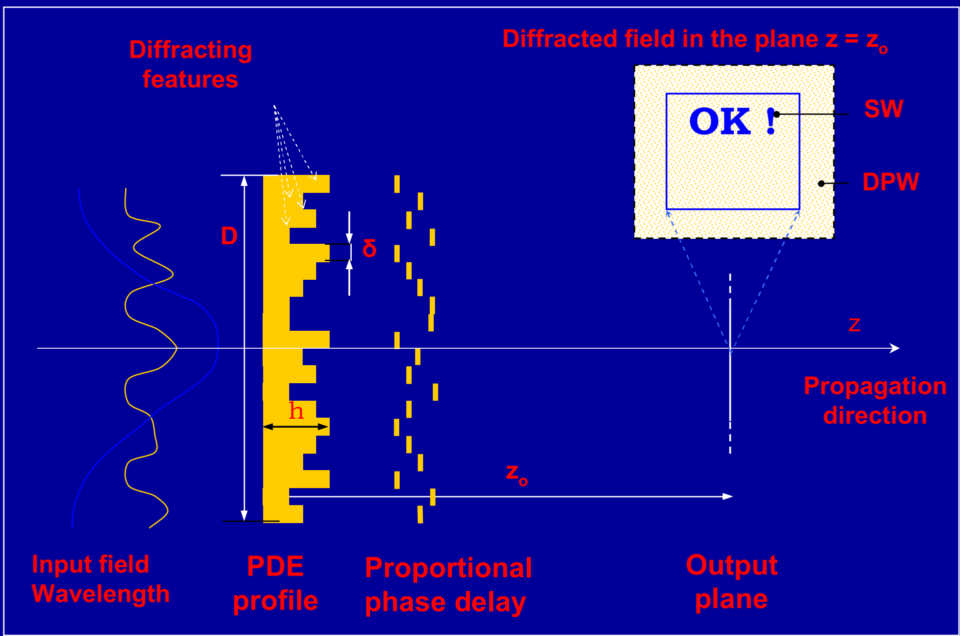

DOE's phase function:

$$\Phi_{DOE}(x) = 2\pi (n-1) h(x) / \lambda$$

Comparison of the iterative algorithms

Intensity distribution

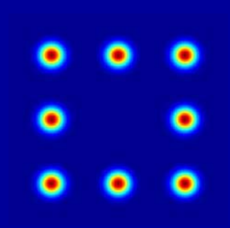

Phase DOE

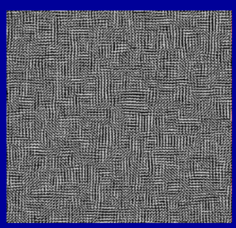

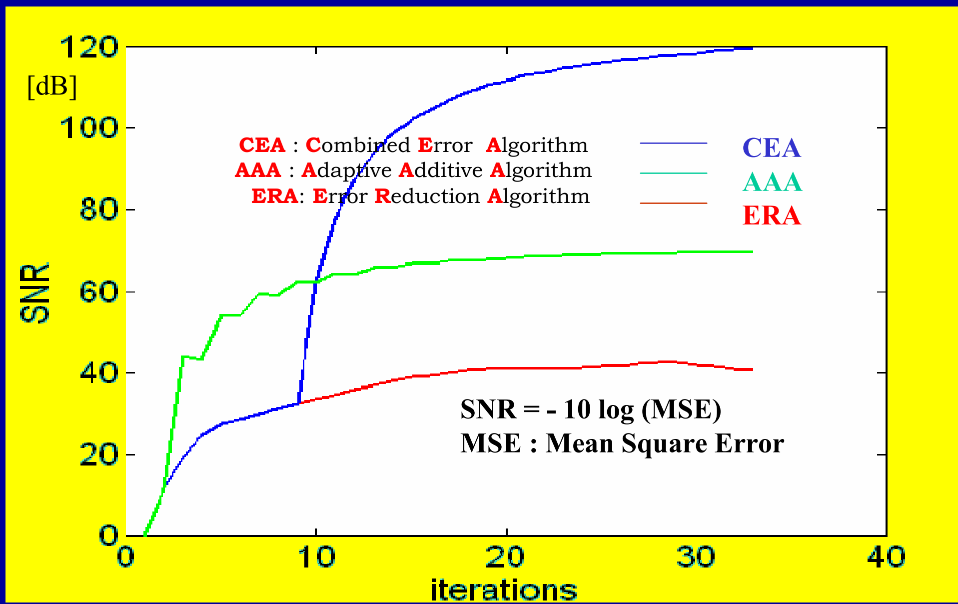

Spherical wave approximation

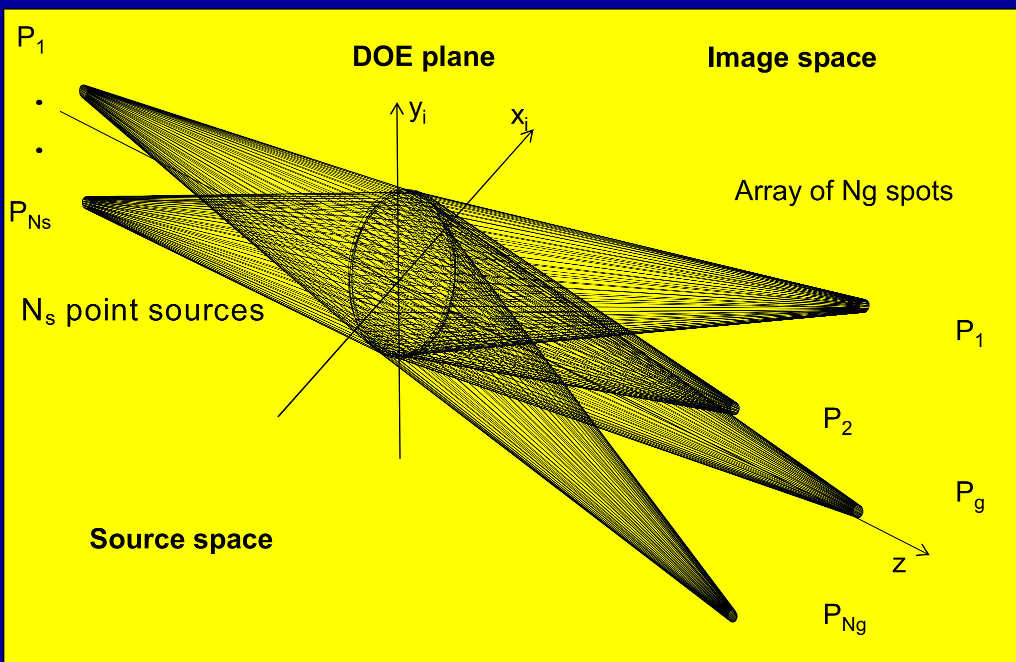

Development of multi-spot X-ray DOE

Optical scheme and calculated layout

of 3 DOE’s that generate 2 and 4

spots (a-b) on the same focal plane,

and 2 spots along the same optical

axis(c)

(d)Full beamshaping

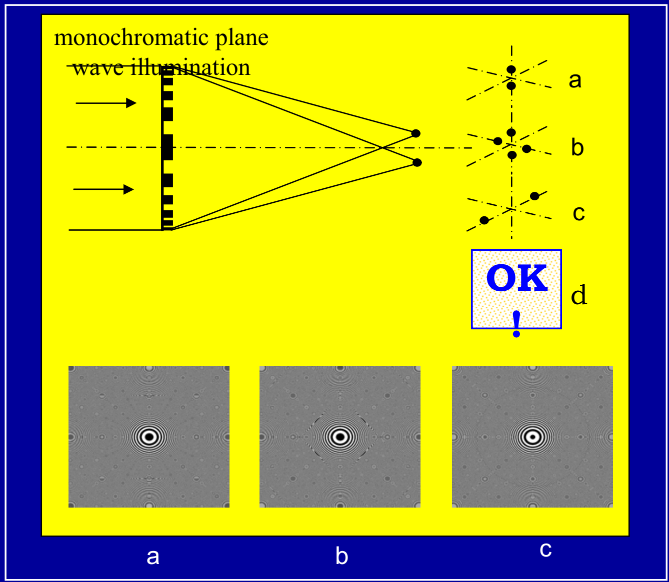

The calculations are referred to a photon energy of 4 KeV and 5 cm focal length

Development of multi-spot X-ray DOE

Calculated pattern of a 4 spot ZP

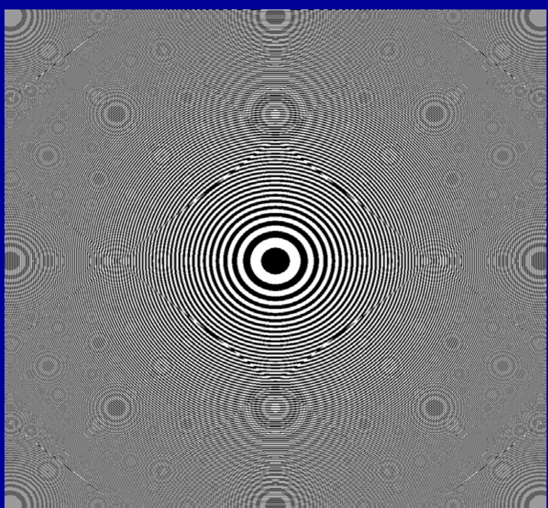

DIC visible light micrograph of 4-spot ZP

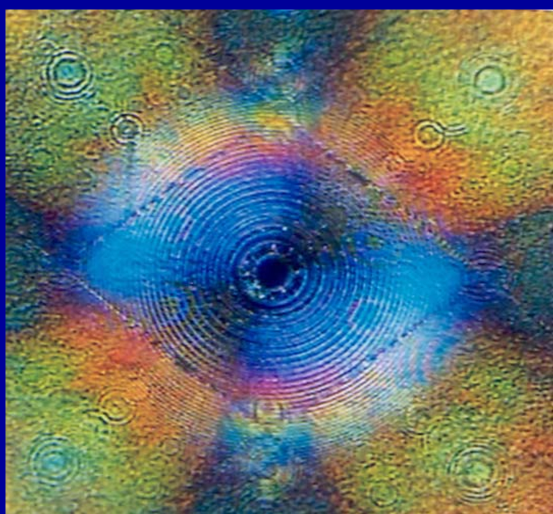

DOE size 0.1 x 0.1 mm2, pixel size: 100 nm, energy 4 keV
designed and generated by the Lilit beamline group (2001)

Development of multi-spot X-Ray DOE

SEM pictures showing an overview of the DOE (DOE area is 100x 100 µm^2) and details of the outermost area whose resolution is below 100 nm

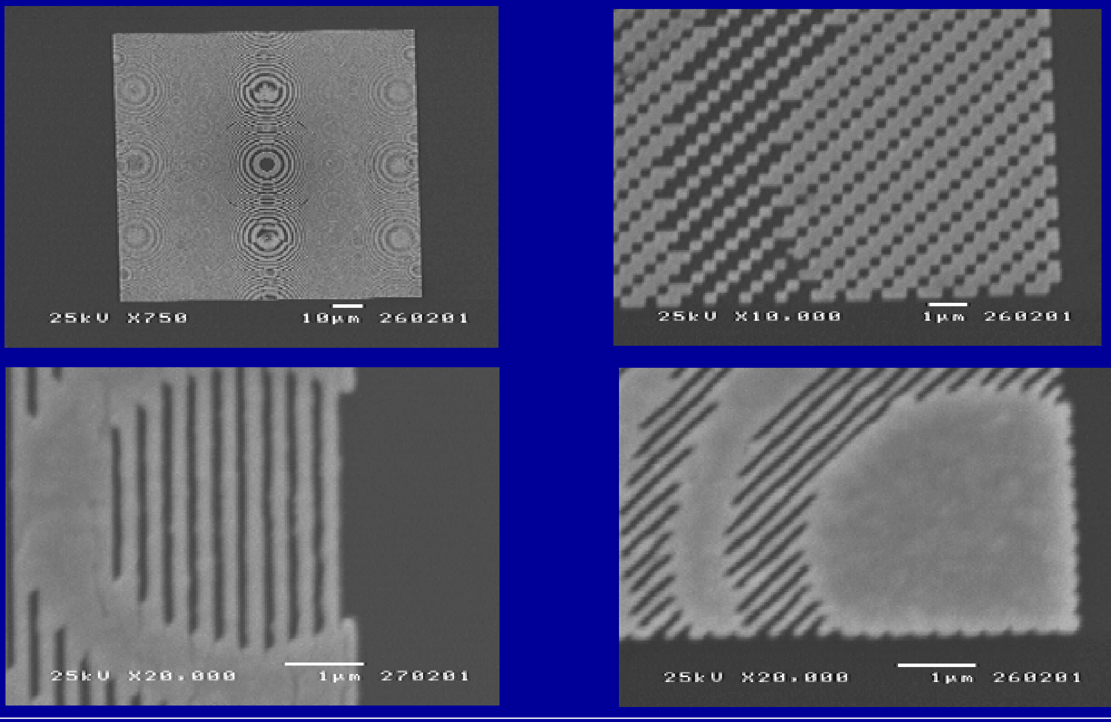

Scanning X-ray microscope at ID21 beamline, ESRF

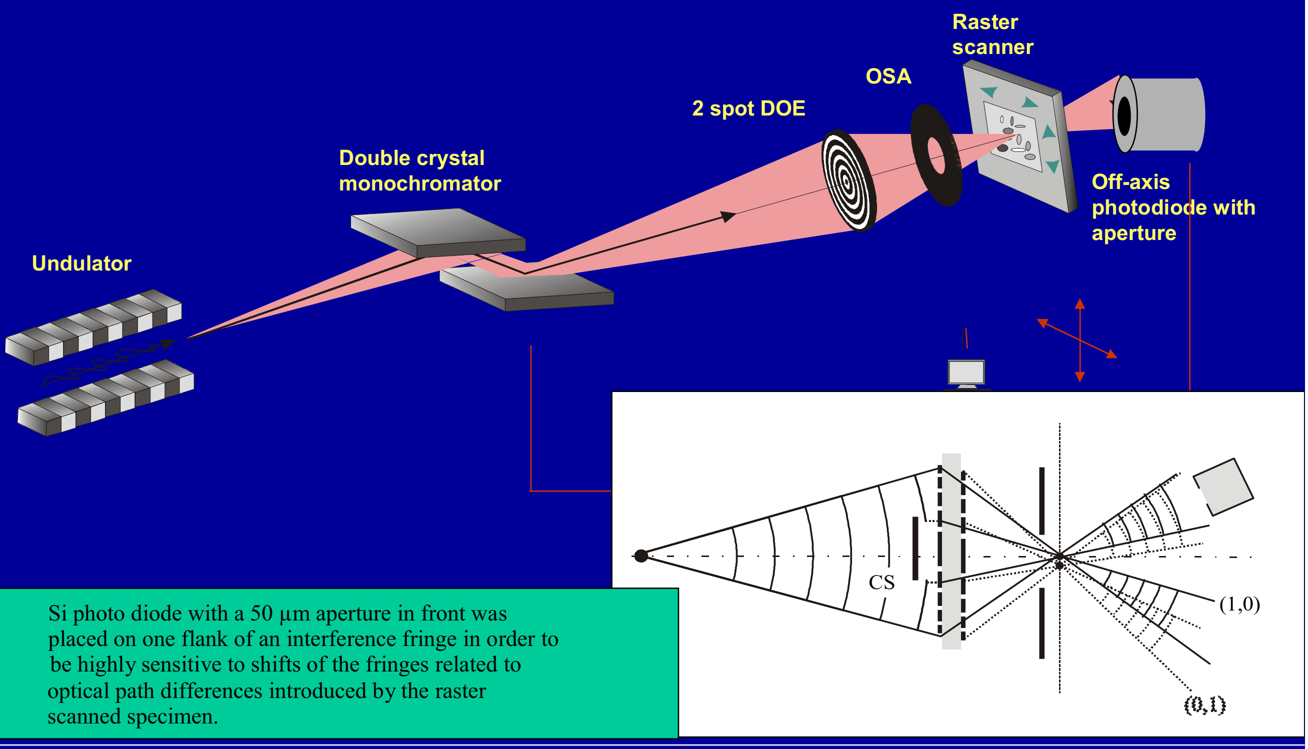

A Si photo diode with a 50 µm aperture in front was placed on one flank of an interference fringe in order to be highly sensitive to shifts of the fringes related to optical path differences introduced by the raster scanned specimen.

2 spot DOE on SXTM at 4 KeV (February 2001)

2 μm thick PMMA test structures
with a transmission of 99 % @ 4 keV

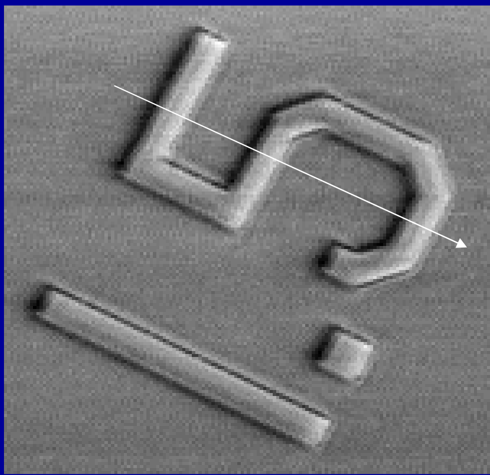

Image taken with the scanning
X-ray microscope at the ID21
beamline, ESRF

Dwell time: 40ms / px
with 200 x 200 px

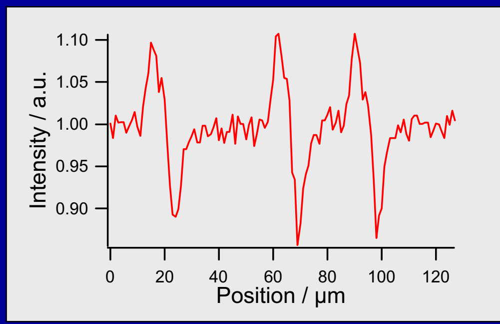

Image contrast: 25% in DIC

Scanning transmission X-ray microscopy in DIC mode using a 2-spot ZP

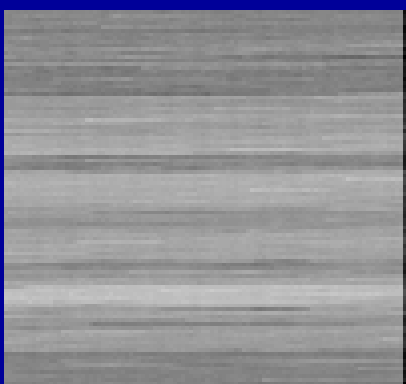

Brightfield (BF)

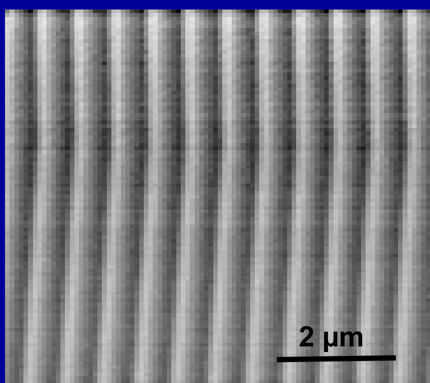

DIC

2 μm thick
grating structures
in PMMA

4 keV

200 x 200 px
40 ms/px dwell

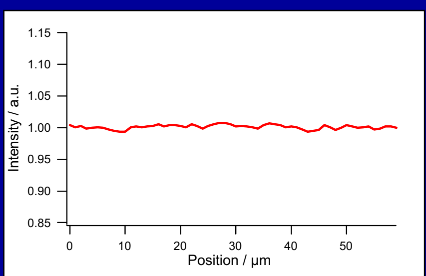

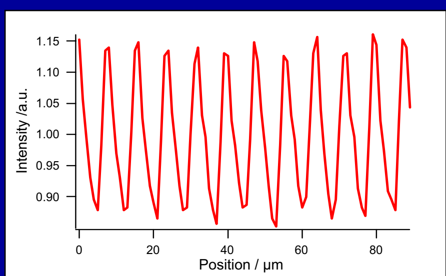

Contrast:

BF: 1 %
DIC: 25 %

ICTP winter college 7-18 February 2005- Trieste

Air Pollution SiO2 fiber Filter(Trieste)
2 spot DIC&XRF measurements (July 2002)

20 µm

7.2 KeV X-ray

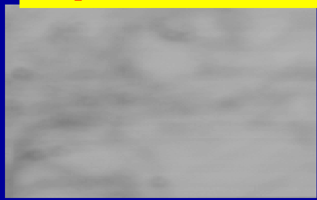
Absorption contrast

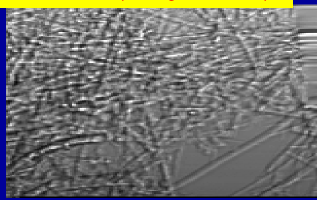
Diff. Interf. contrast

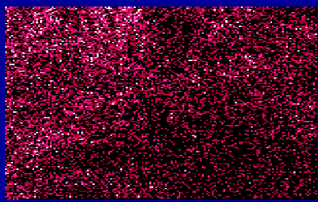
Cr XRF map

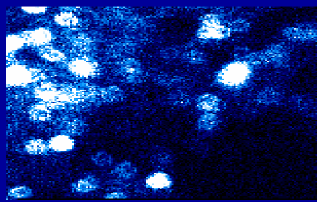
Fe XRF map

4 KeV X-ray

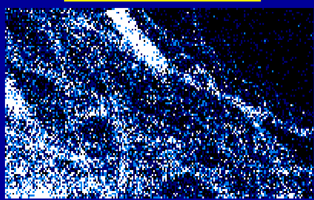
Ca XRF map

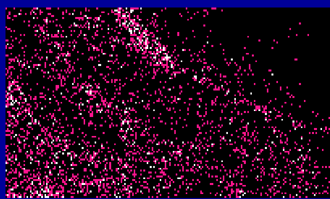
K XRF map

Optical setup of DIC full field microscope

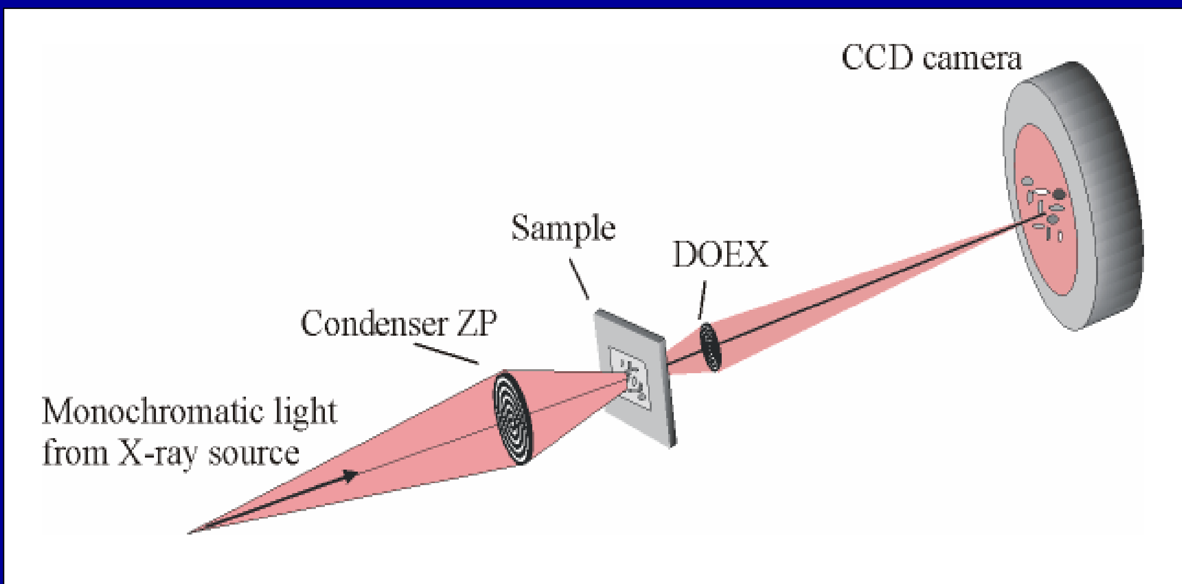

PMMA test structures (June 2001)

test structures(a=squares, b=toroids) 1 µm thick with a transmission of 99.99 % @ 4 keV

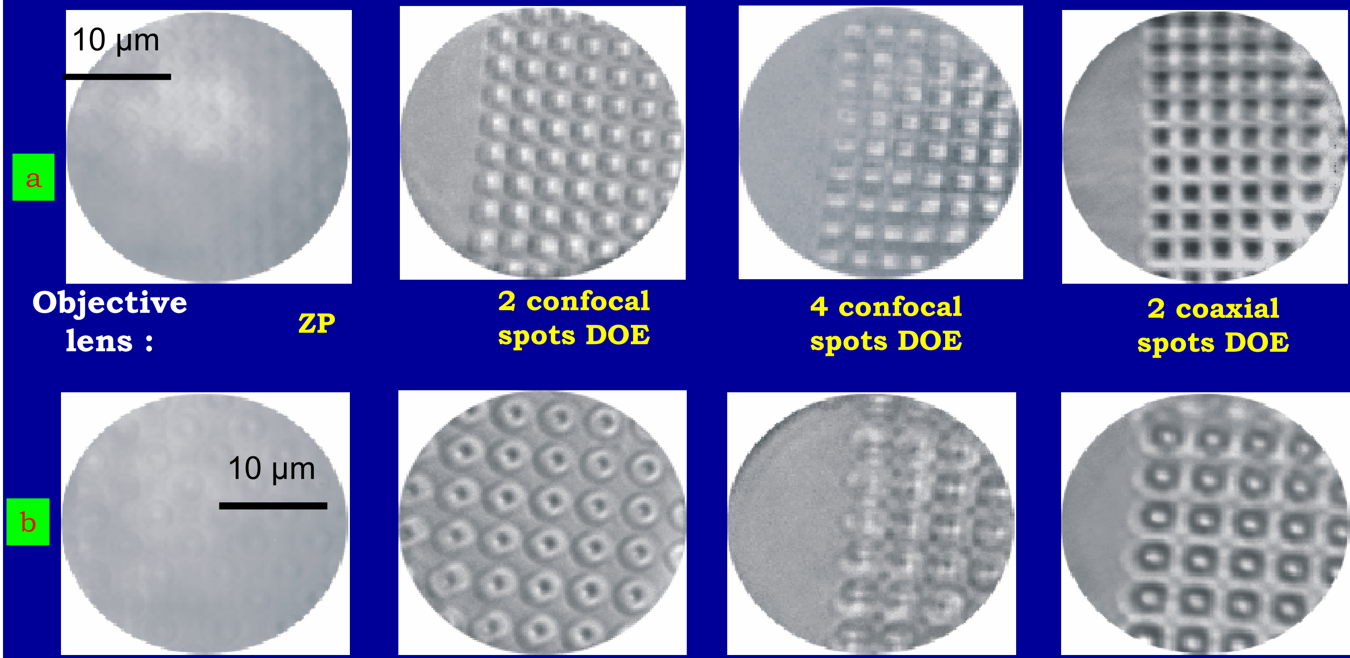

Yeast cells: imaging in TXM at 4 keV

by using diffractive optics

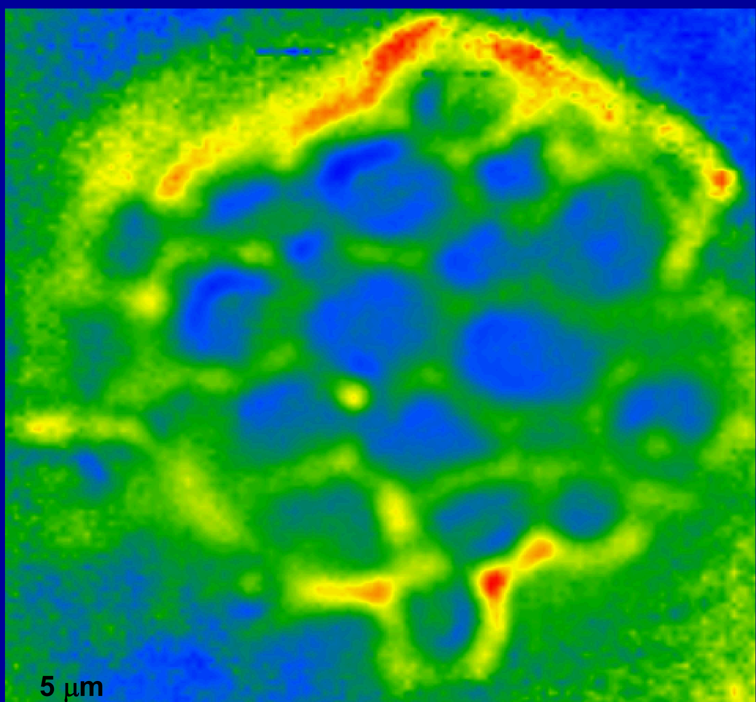

Complete X-ray- beam shaping

Optical setup of DIC full field microscope

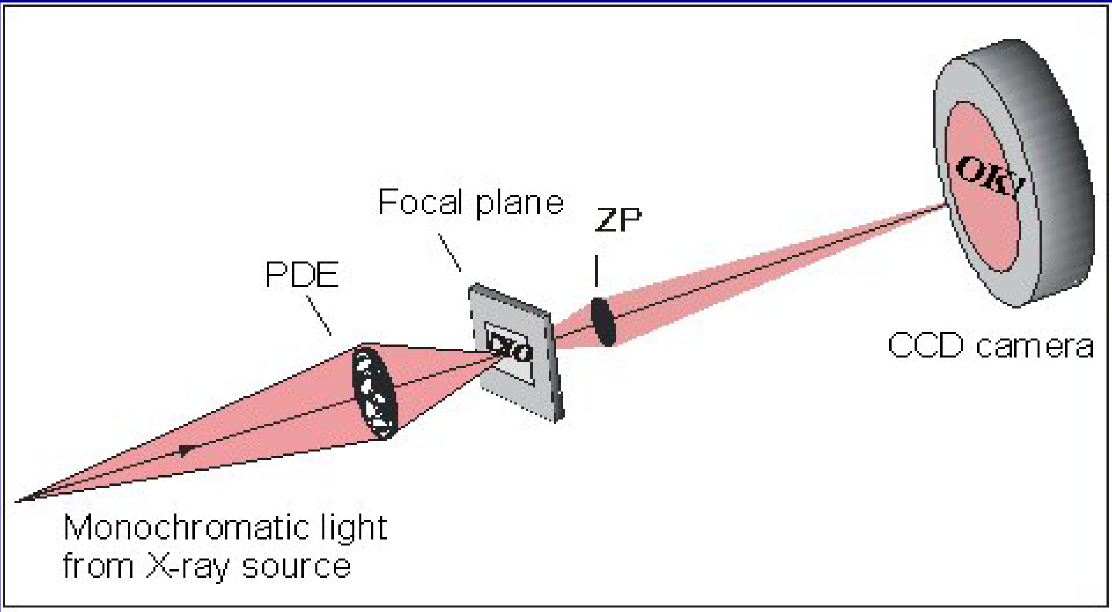

Complete X-ray- beam shaping (June 2001)

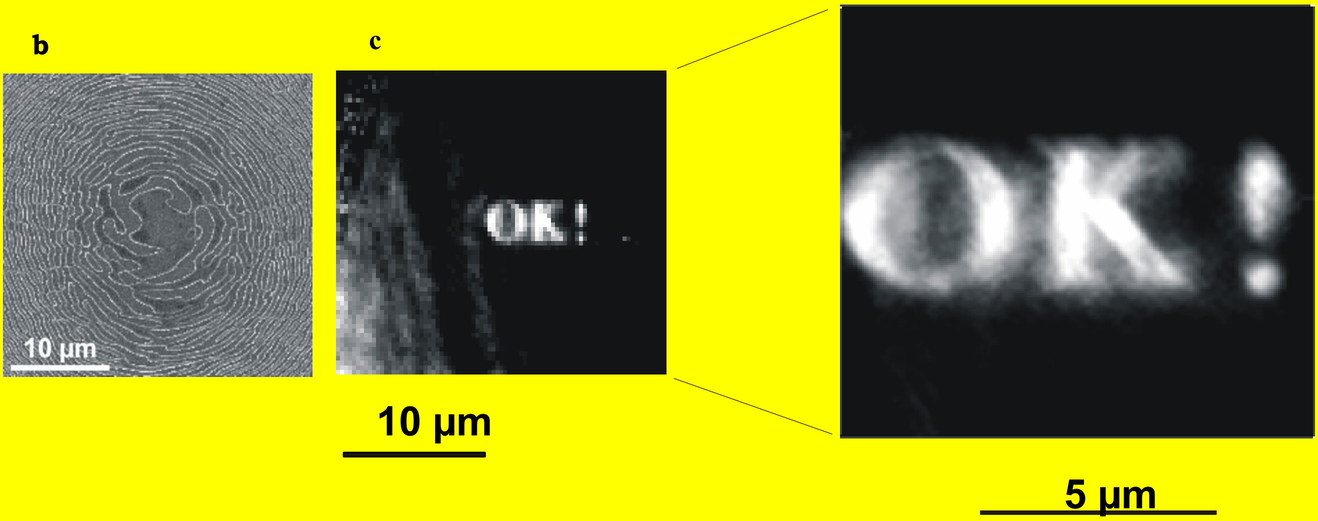

b - SEM image of the fabricated OK! DOE
c - The intermediate image formed by the DOE at the focal plane located at 50 mm is magnified 150 times on a CCD detector by a ZP that acts as an objective lens

DIC Image formation with coherent illumination

$$i(\boldsymbol{x}) = a_1 \left| \int_{-\infty}^{+\infty} f(\boldsymbol{x_o})\, h(\boldsymbol{x} - \boldsymbol{x_o})\, d\boldsymbol{x_o} \right|^2$$

$f(\boldsymbol{x}) = \exp(-j\phi(\boldsymbol{x}))$ **Transmission function of the phase object**

$$h(x,y) = 0.5\,\exp(-j\Delta\theta)\delta(x-\Delta x, y) - 0.5\,\exp(j\Delta\theta)\delta(x+\Delta x, y)$$

$h(x,y) =$ **Ideal PSF from ray-tracing (geometrical optics)**

Δx **=Shear in x direction**

$\Delta\theta$ **=constant phase bias**

C. Preza et. al. *J. Opt. Soc. Soc. Am. A/Vol. 16, No. 9. 1999*

Field Intensity in the DIC image

$$i(x,y) = a_1 \sin^2\left[0.5\left\{\phi(x-\Delta x, y) - \phi(x+\Delta x, y)\right\} + \Delta\theta\right]$$

If the shear Δx **very small (differential) comapared to the size of the details of the specimen (or the resolution of the ZP) ==> the phase difference can be written as a phase gradient:**

$$i(x,y) = a_1 \sin^2\left(\Delta x \frac{\partial\phi(x,y)}{\partial x} + \Delta\theta\right)$$

With DOE is possible to control the contrast through the bias $\Delta\Theta$

Bias retardation in DIC

$$i(x,y) = a\sin^2\left(\Delta x\frac{\partial\phi(x,y)}{\partial x} + \Delta\theta\right)$$

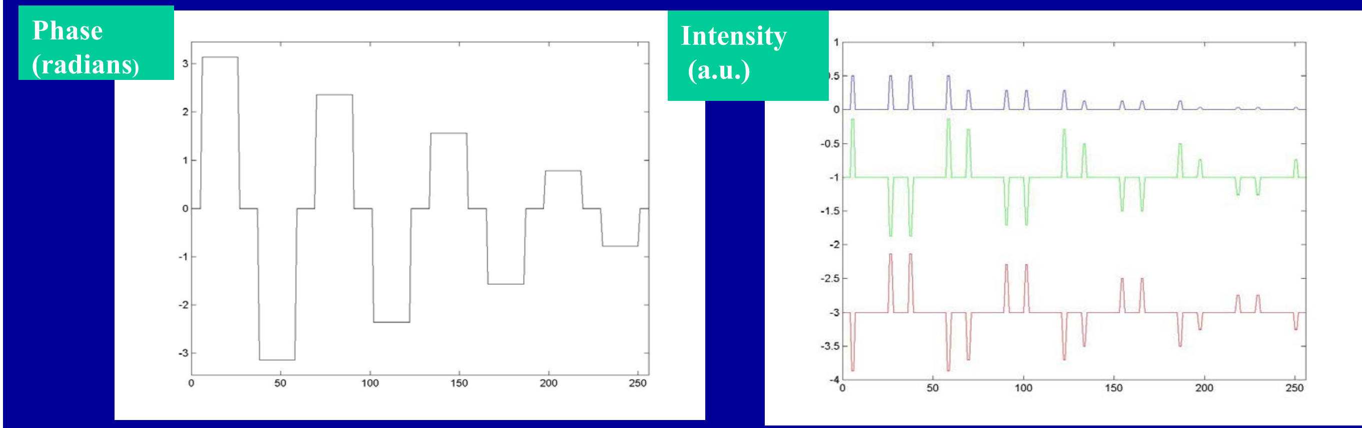

(a) The phase function of a one dimensional object described in 250 pixels;
(b) Intensity distributions obtained with the same shear $\Delta x = 2$ but different bias values: $\Delta\theta = 0$ - first line, $\Delta\theta = \pi/4$ - second line, and $\Delta\theta = 3\pi/4$ - third line;
the signals are offset by 2 a.u. for a clear representation

Spherical wave propagation approach

To calculate the phase function Φ_{PDE}, we assume that the light source which illuminates the PDE and the intensity distribution produced by the PDE can be described by point sources generating spherical waves

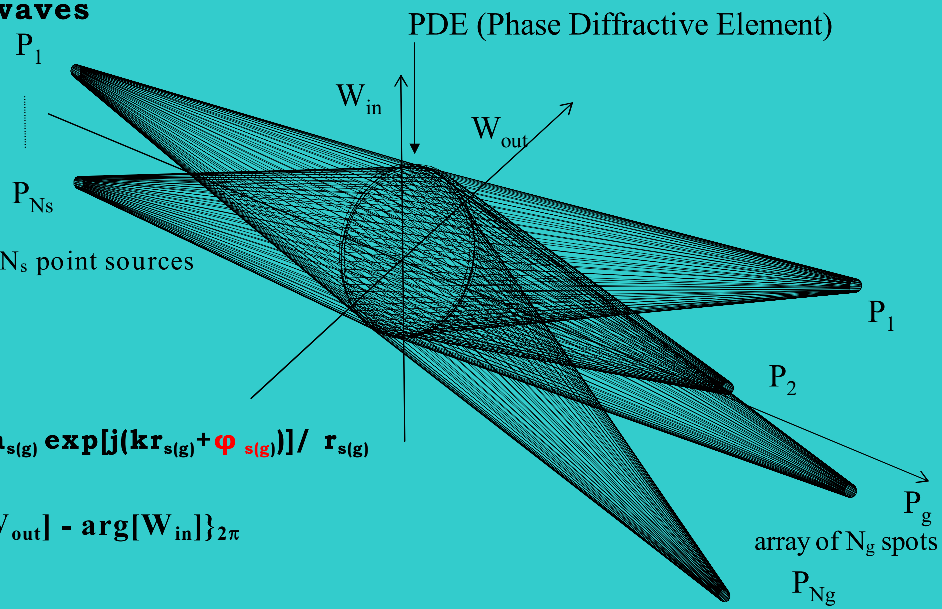

$$W_{in(out)} = \sum_{s(g)} a_{s(g)} \exp[j(kr_{s(g)} + \varphi_{s(g)})] / r_{s(g)}$$

$$\Phi_{PDE} = \{\arg[W_{out}] - \arg[W_{in}]\}_{2\pi}$$

DOEs producing the same beam shearing (1 mm) but different bias: a) no bias, b) bias = π at 1 m from the DOE (DOE size= 2 cm, described in 480 pixels)

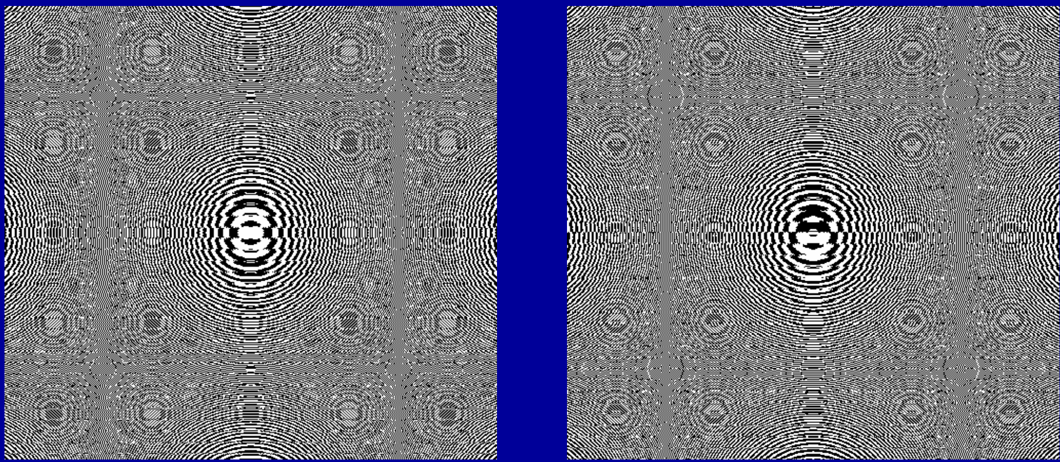

The intensity distribution obtained in the focal plane (Δx=1 mm λ=532 nm DOE made by Hamamatsu SLM)

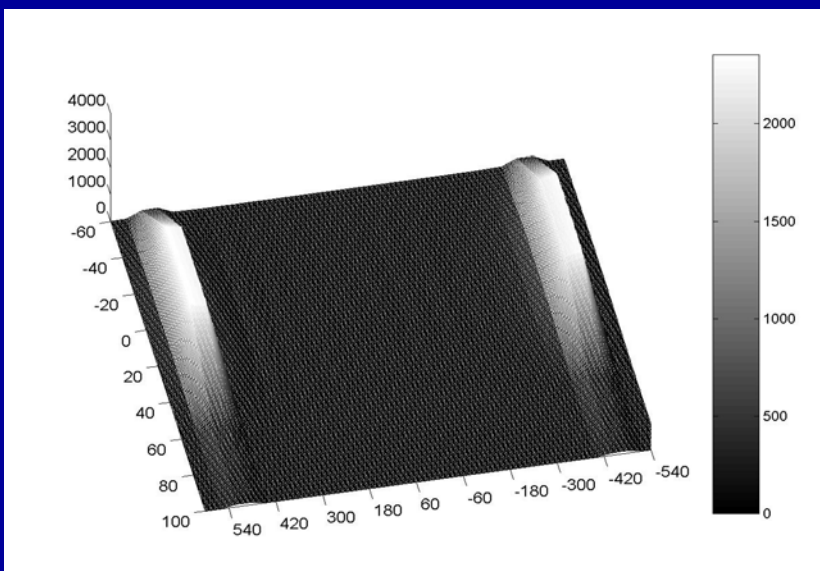

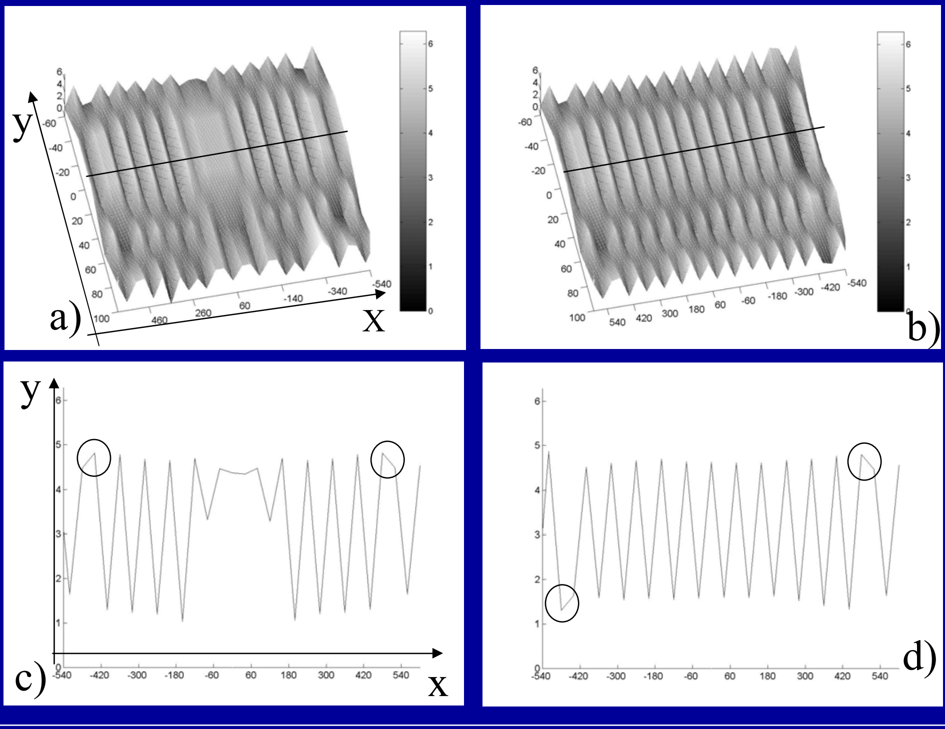

Phase distributions obtained in the focal plane of the DOE. For the 3D graphics (a,b) the phase is represented in radians on the z axis, the distances represented on x and y axes being expressed in microns. The phase distributions along the lines indicated in a) and b) are represented in the second line c) and d) clearly showing the presence of the π bias

The interference patterns obtained after the focal plane of the DOEs implemented on the phase SLM Hamamatsu;
the left pattern corresponding to the DOE without bias is shifted with half of a fringe with respect to the right pattern which corresponds to the DOE with bias π

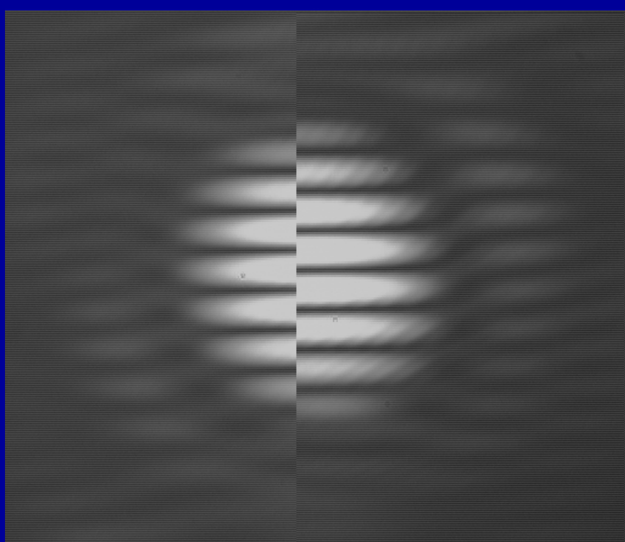

Complete set of objectives and condenser lens fabricated By e-beam lithography

2 spots at 6.5 KeV 50 nm res.

2 spots at 2.5 KeV 50 nm res.

Top hat condenser at 4 KeV 150 and 200 nm res.

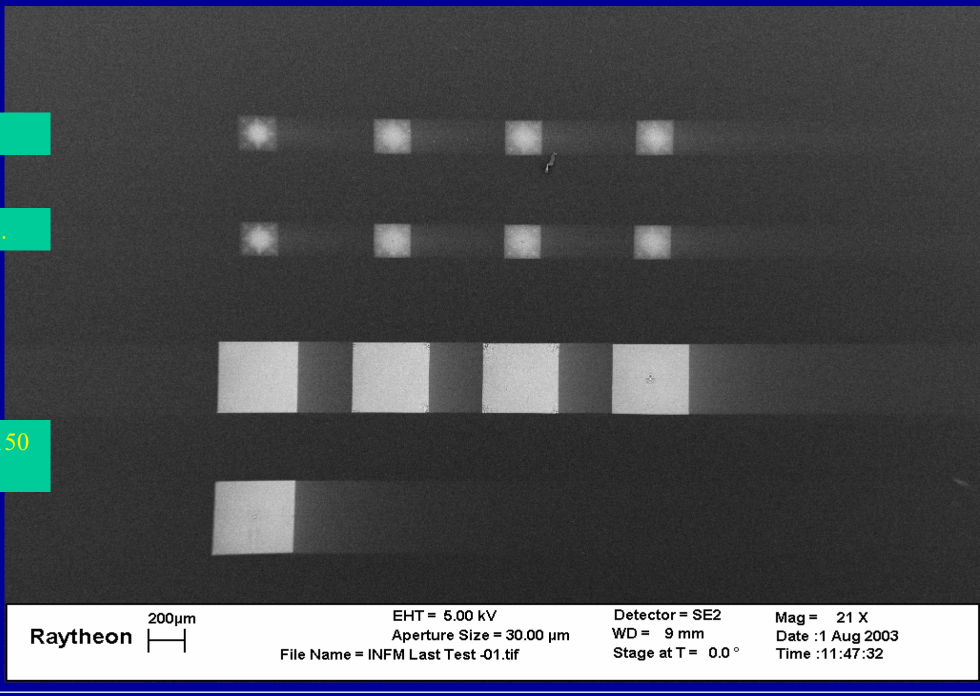

DOE for Bias control

$\Delta\Theta=0$

$\Delta\Theta=\pi/2$

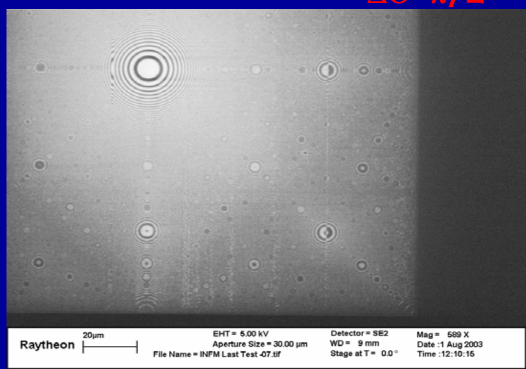

$\Delta\Theta=\pi$

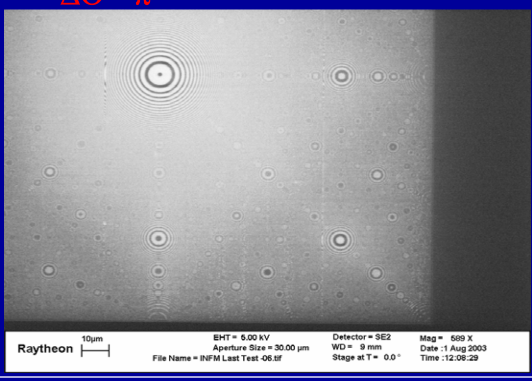

$\Delta\Theta=2\pi/3$

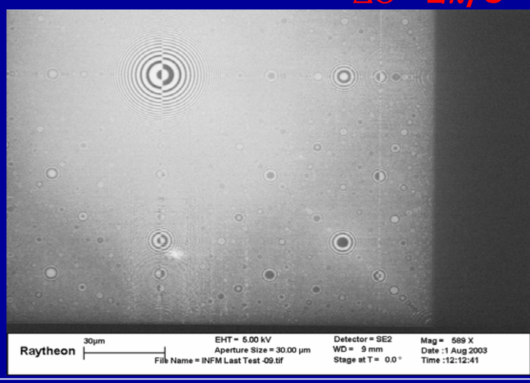

Top Hat at 4 KeV 25.6 microns field of view (DOE res. 150 nm)

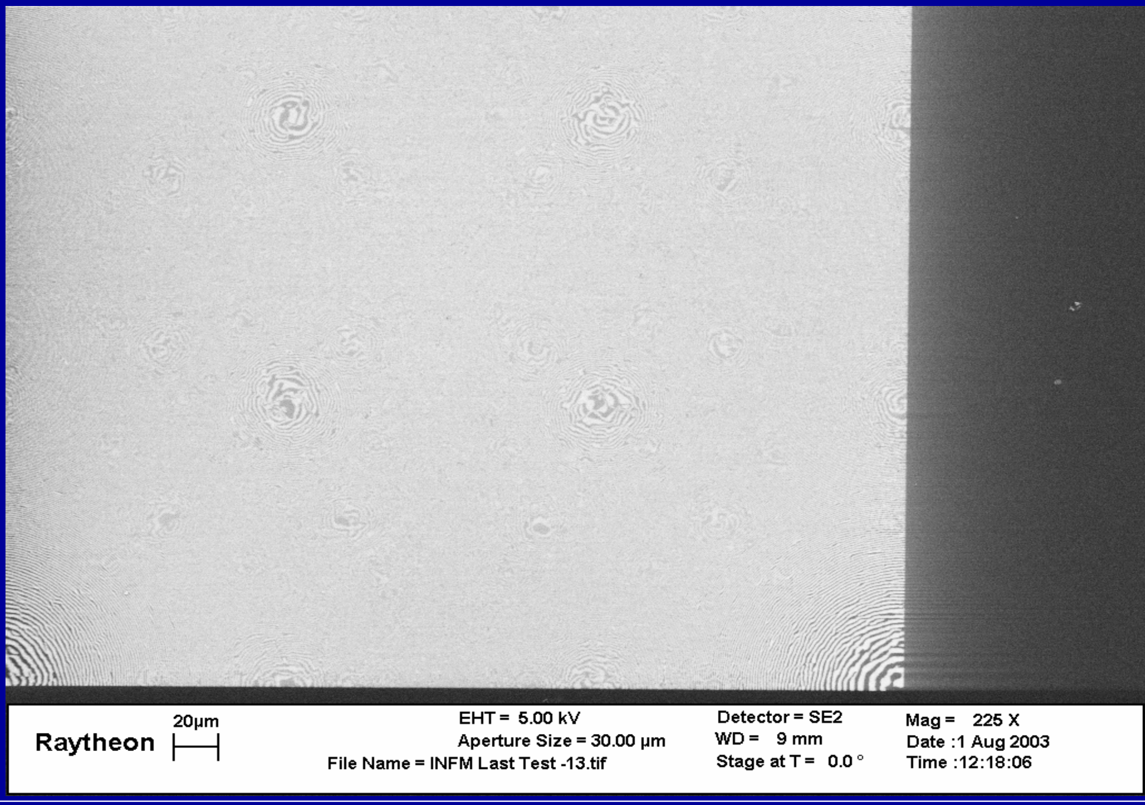

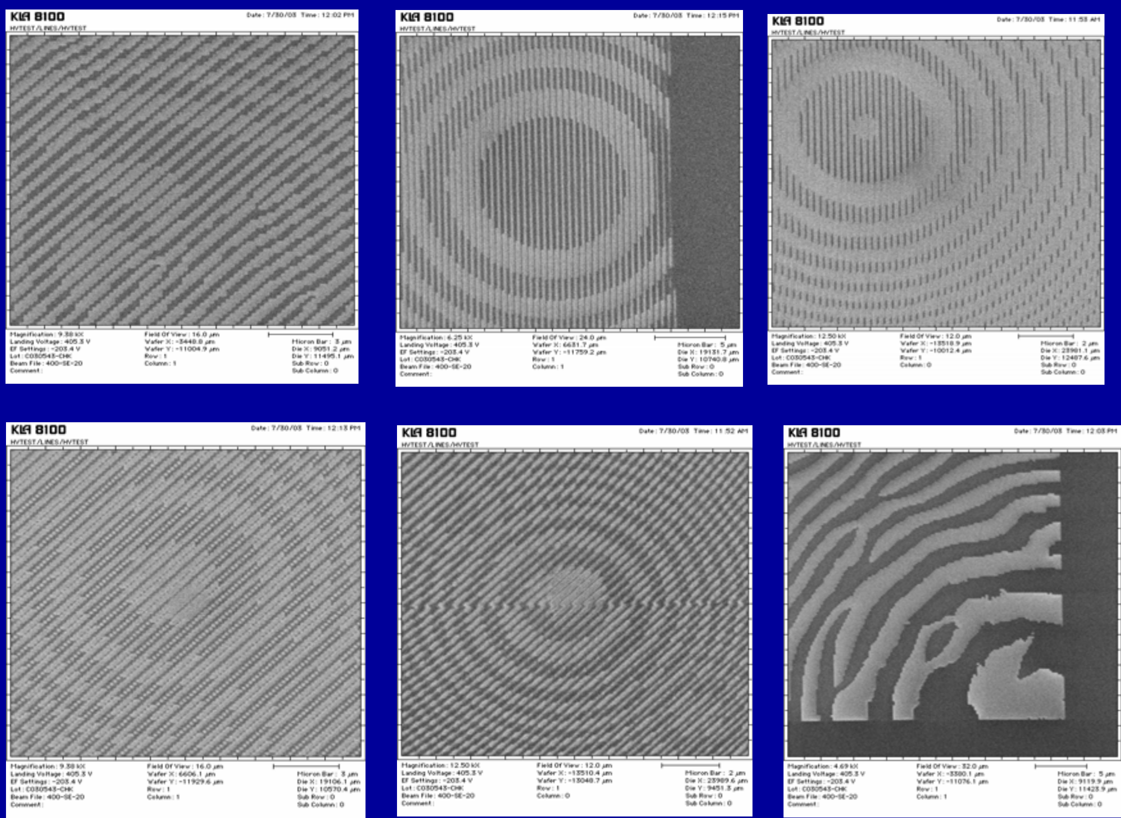

Further DOE already fabricated to be tested

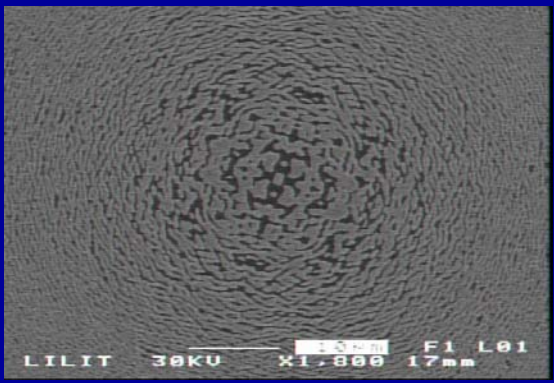

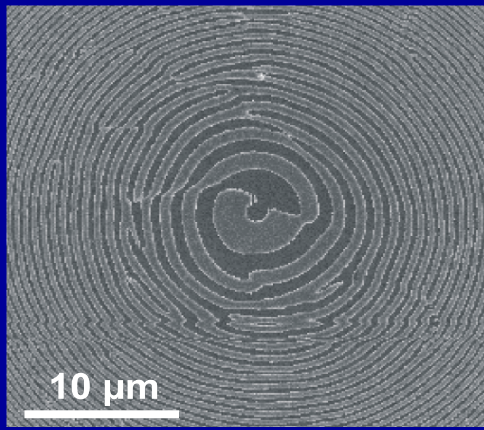

- Top Hat for TXM microscope (to replace the conderser lens)
- New annular distribution for DIC microscopy
- Sub micron Intensity pattern for maskless lithography and CVD induced by X-rays

50 nm smaller pixel size with 30 nm details

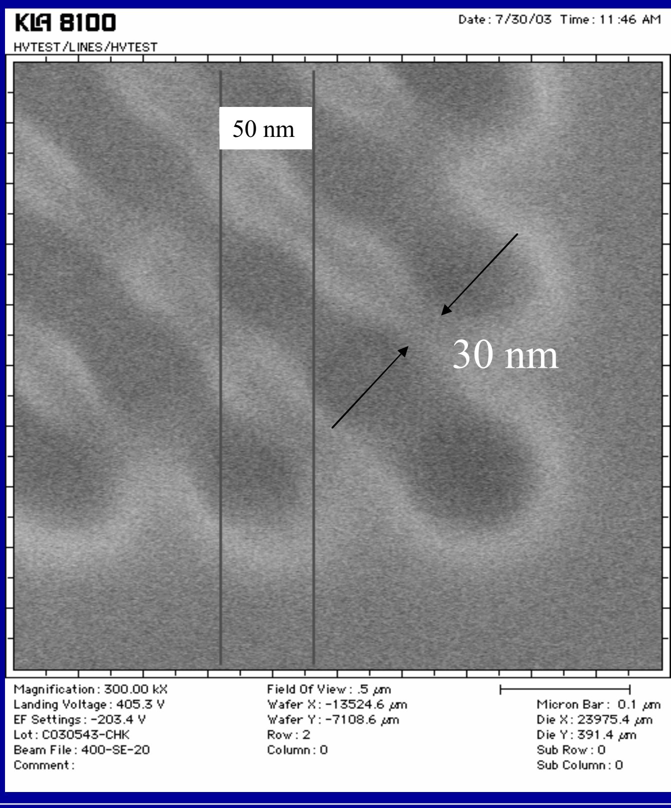

Experimental results DOE for XRM

From the report
DOE Experiment
O. Dhez and M.Salom´e
7/10/2003

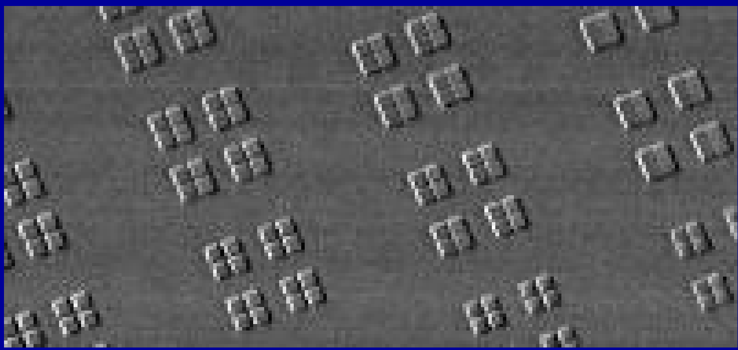

Experiment performed on ID21 SXM branch, in 16 bunch mode, under vacuum at 6.5keV. The sample used is the PMMA test object.

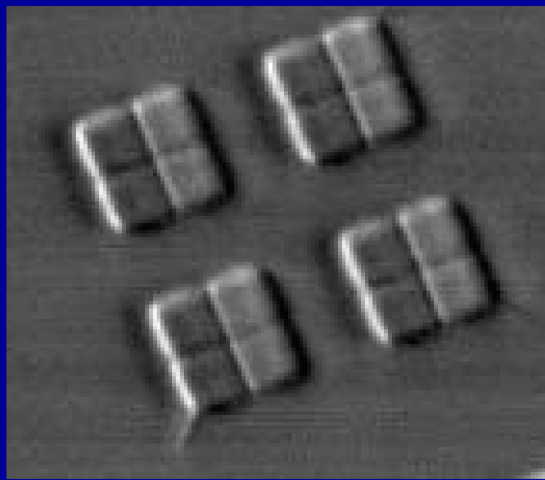

Air Pollution SiO2 fiber Filter(Trieste)
2 spot DIC&XRF measurements (July 2002)

7.2 KeV X-ray

Absorption contrast

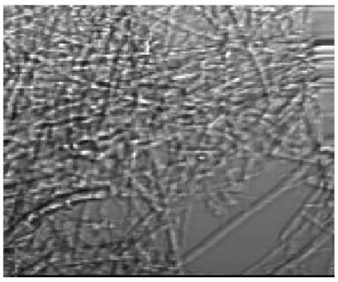

Diff. Interf. contrast

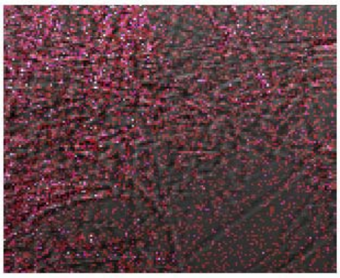

Cr XRF map

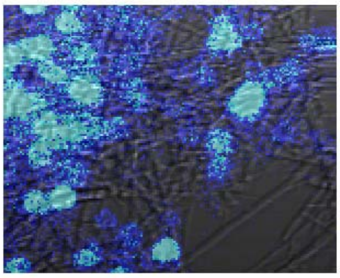

Fe XRF map

Id21, ESRF, Mi578, 7.2 keV, 160 x 145 (?) px, 100 x 100 µm
thin sample

4 KeV X-ray

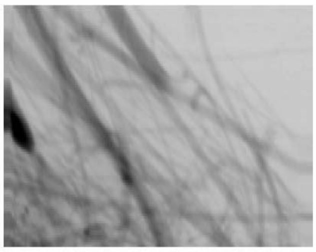

Absorption contrast

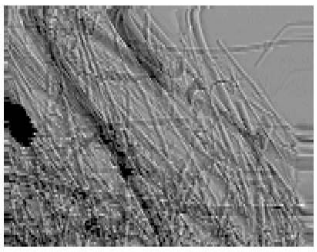

Differential interference contrast

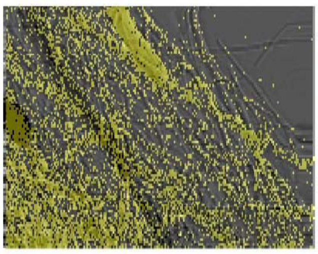

Ca XRF map

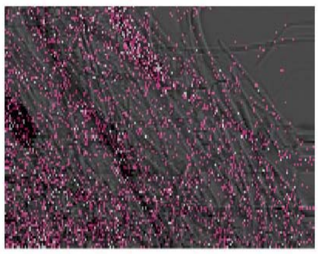

K XRF map

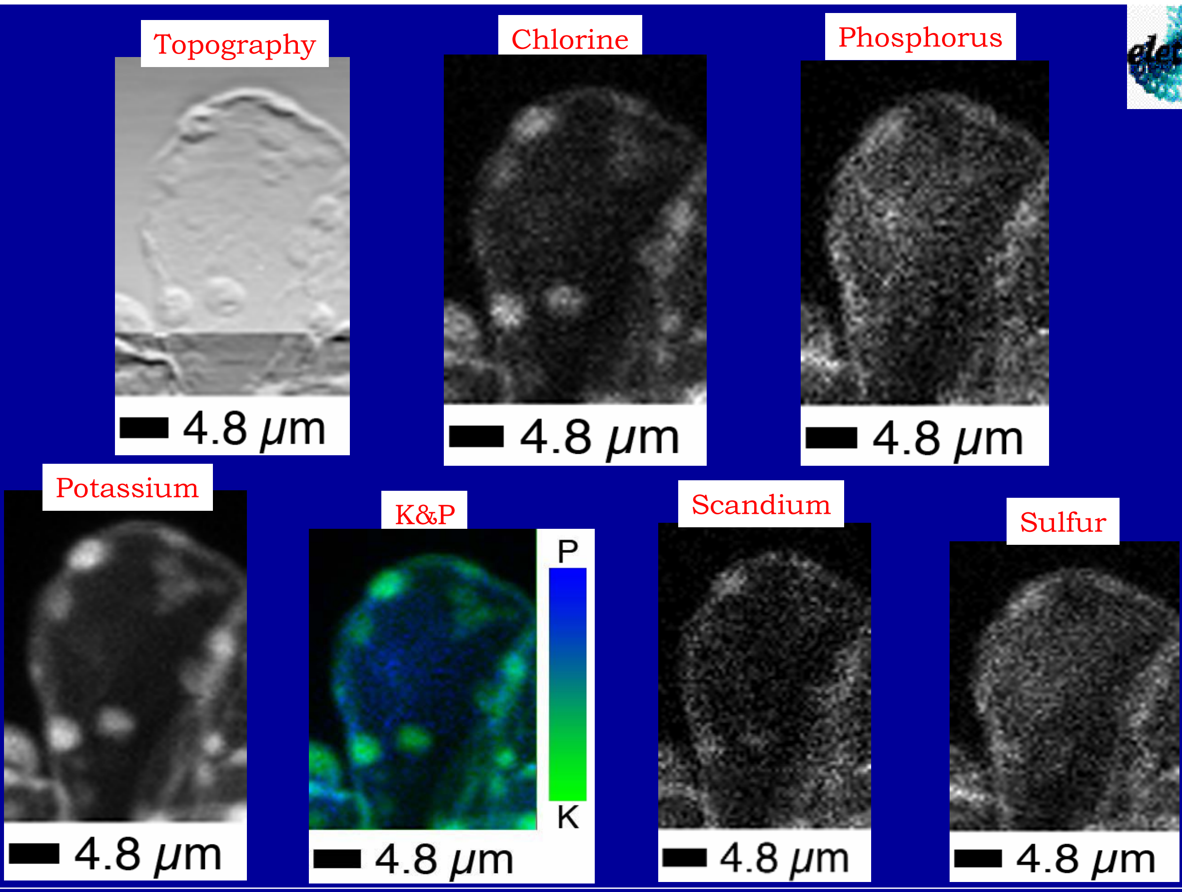

LEO 1540XB CrossBeam

System Features:

- Super Eucentric 6-axis stage
  X 102 mm, Y 102 mm
- Gas injection system
- 4“ Airlock (optional)
- Automated aperture change on FIB column
- Enhanced vacuum system

Optional incuded:

- EDS
- CAD
- Lithography
- SIMS

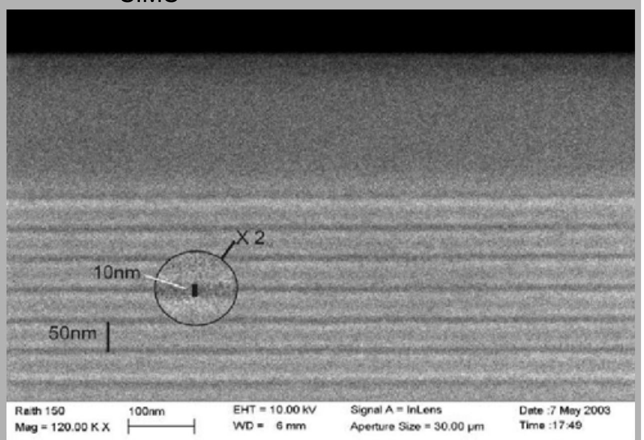

NanoImprinting

Stamp materials : Si, Si oxide, Si nitrate,Ni, W, quartz, sapphire

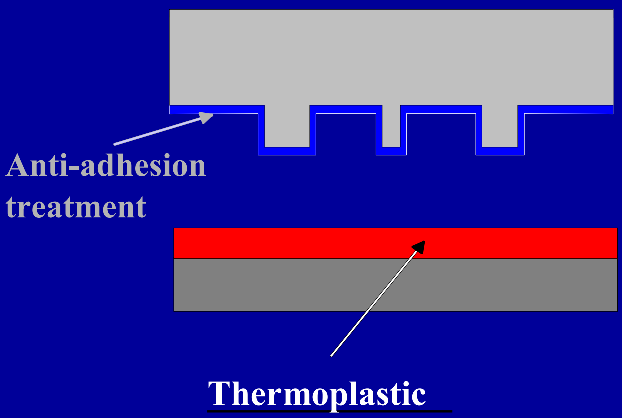

Embossing conditions

pressure: 50-100 bar

temperature: T ~ T_g + 90°

Patterning large features by Nanoimprint

Master: Gold on Silicon

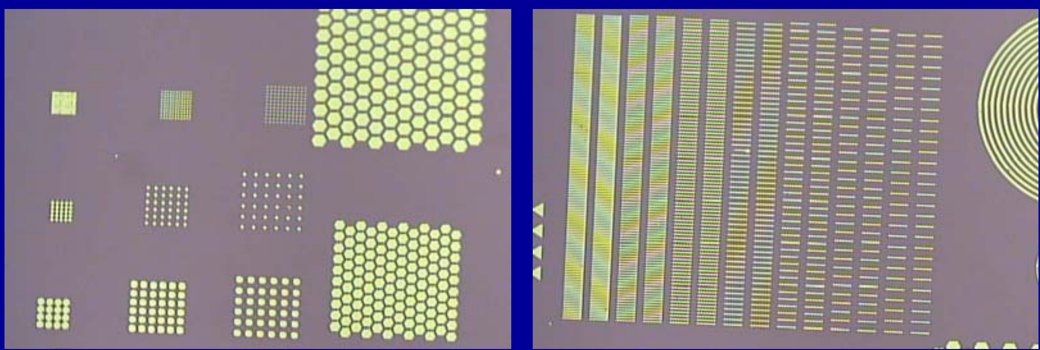

Imprinted structures: PMMA (plexiglass) on Silicon

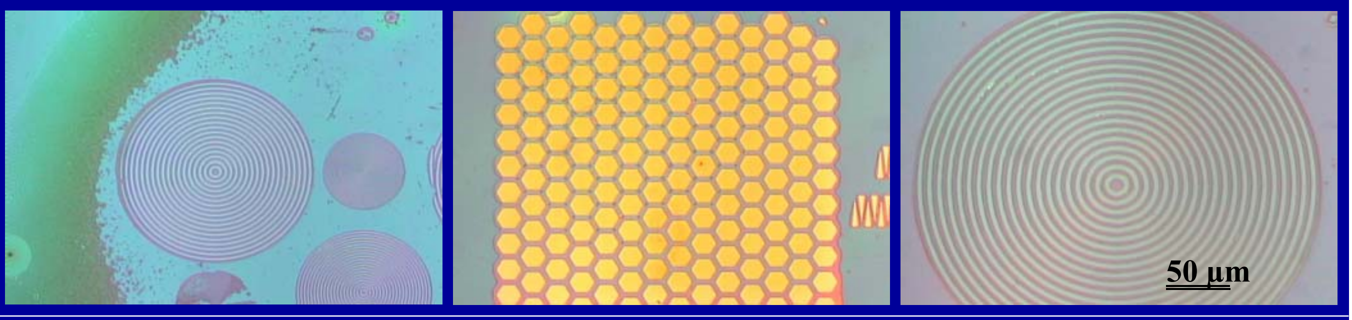

Outlook and future investigations

- ✓Two different DIC techniques using ZP doublet and X-Ray DOE
- ✓Spatial resolution according to the design
- ✓Technique has no limitation in spectral range as far as ZPs can be applied
- ✓Full beam shaping achieved at X-ray wavelength

Future investigations:

- ➢Extension of experiments to soft and harder X-rays
- ➢Resolution limit toward state-of-art- fabrication technique
- ➢Theoretical investigations and simulations (transfer function)
- ➢ Combination with spectro-microscopy for biological sample

Acknowledgements

Lisa Vaccari, Matteo Altissimo, Luca Businaro
TASC-INFM at ELETTRA, Lilit

B. Fayard, U. Neuhaeusler, M. Salome, R. Baker
ESRF, ID21, Grenoble, France

F. Polack, D. Joyeux,
Lure& Universite Paris-Sud, Orsay, France

Alexei Barinov, Maya Kiskinova
ELETTRA

Basic properties of zone plates

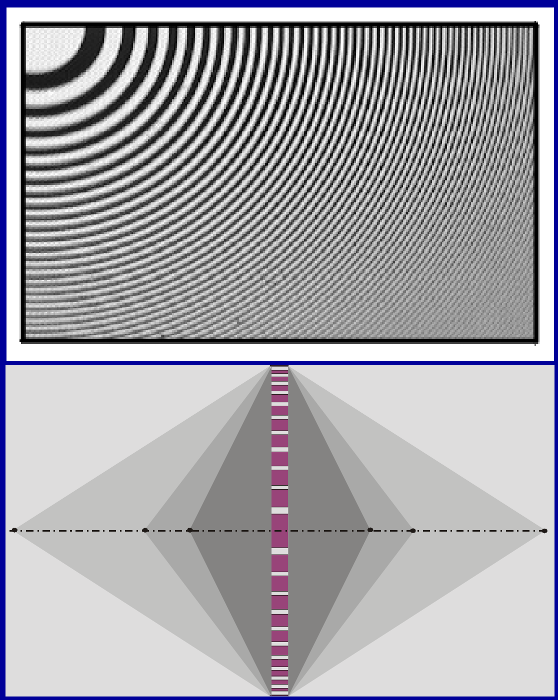

Focusing, circular diffraction grating with radially increasing line density

$$\frac{1}{f} = \frac{1}{p} + \frac{1}{q} \qquad \text{if} \quad n > 100$$

In terms of ZP parameters:

$$f_m = \frac{2}{m} D\, dr_m / \lambda$$

To avoid chromatic aberrations:

$$\frac{E}{\Delta E} \geq n\, m$$

$$\delta_m = [\, \delta_{i,m}^2 + \delta_r^2 + \delta_c^2\,]^{1/2} = [\, (1.22 \cdot dr_n / m)^2 + \delta_r^2 + (D \cdot \Delta E/E)^2\,]^{1/2}$$

Phase – retrieval iterative algorithms

ERA: **E**rror **R**eduction **A**lgorithm, Aoi = Ao; DFW = SW

AAA : **A**daptive **A**dditive **A**lgorithm, Aoi = λAo+(1- λ)Aot inside SW; DFW > SW

CEAA : **C**ombined **E**rror **A**daptive **A**lgorithm

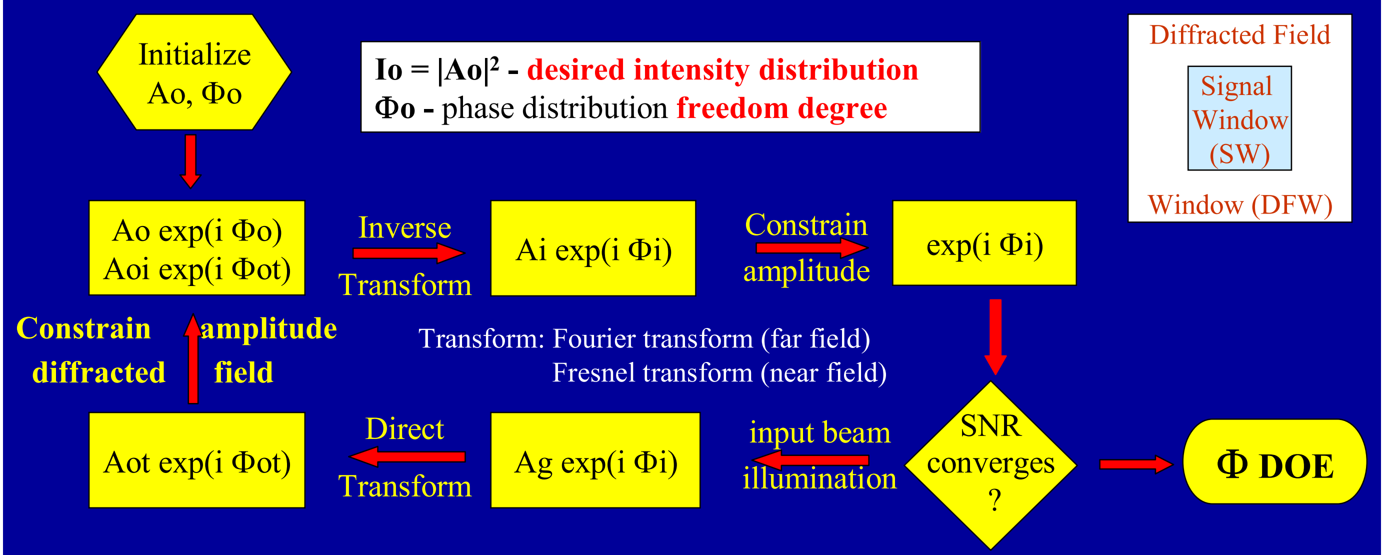

Scalar diffraction based model

scalar diffraction theory

$$d \succ 3\lambda$$

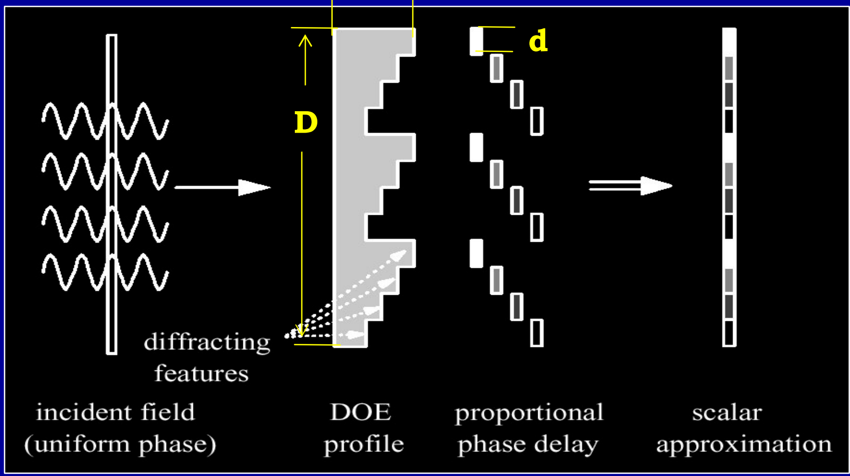

DOE's phase function:

$$\Phi_{DOE}(x) = 2\pi\,(n-1)\,h(x)\,/\,\lambda$$

Coherence considerations

Spatial coherence (Van Cittert-Zernike)

$$D = 0.61 \frac{L\lambda}{d/2} = 1.22 \frac{f\lambda}{\delta}$$

D: Diameter of coherently illuminated plane
d: Source diameter
L: Distance to observation plane

ZP shift $\Delta x < \delta = 1.22\, dr_N$

Then:

If the separation(Δx) of the two superimposed images is below the resolution limit (δ) the two images will interfere without further restrictions to the spatial coherence of the source or, DIC works independent, of the spatial coherence of the illumination

Temporal coherence

$$l_{coh} = \frac{\lambda^2}{2\,\Delta\lambda} > \frac{\lambda}{2} N = \Delta s_{max}$$

l_{coh}: coherence length
Δs_{max}: path length difference
N: Number of zones

$$\frac{\lambda}{\Delta\lambda} > N \approx N_{eff} = \frac{(r+\Delta x)^2}{\lambda f}$$

ZPs have to be treated to be in the same plane (within their depth of focus) (N>100)

Then:

No precautions to the source spectrum or other than for imaging with a single ZP

DIC X-ray microscopy with a full-field imaging microscope @ 4 keV

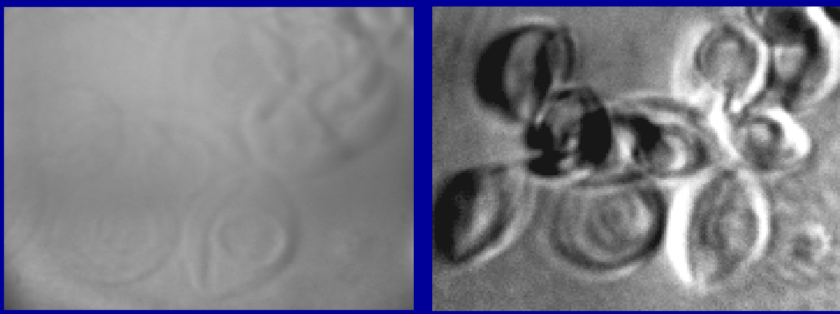

Spores of giant moss "Dawsonia superba"

Exp. time: 20 s

5 μm

Wing of a moss

Exp. time: 30 s

10 μm

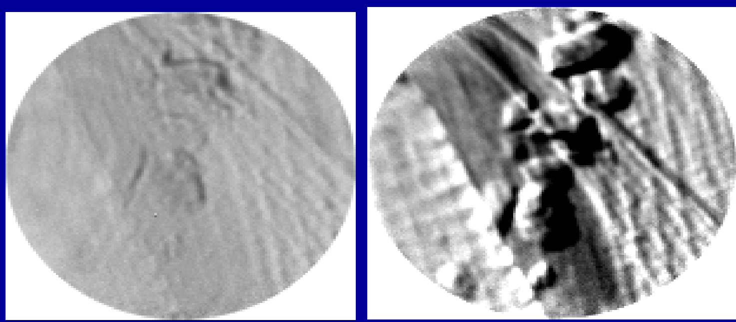

B. Kaulich, T. Wilhein, E. Di Fabrizio, S. Cabrini, F. Romanato, M. Altissimo, J. Susini (Nov 2000)

Summary of DIC with ZP doublets

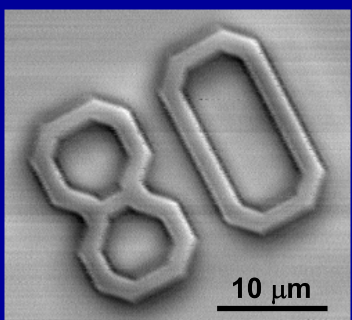

- **DIC contrast technique, which is applicable for photon energies where ZPs work successfully (0.1 – 30 keV)**
- **Increase in image contrast of up to 20x – 30x achieved**
- **Method can for the first time be applied in both transmission X-ray microscopy types (STXM *and* TXM)**
- **Alignment procedure not more complicated than for a single ZP**

Improvements on ZP doublets fabrication:

- **Simpler nanofabrication process (X-ray litho)**
- **Optimization in ZP diffraction efficiency (10 % @ 4 keV meas.)**
- **Improvement in spatial resolution**
- **higher energy range accessible > 10 keV**

Full-field imaging microscope operating in DIC mode – Optical setup

Full-field imaging microscope at ID21 beamline, ESRF

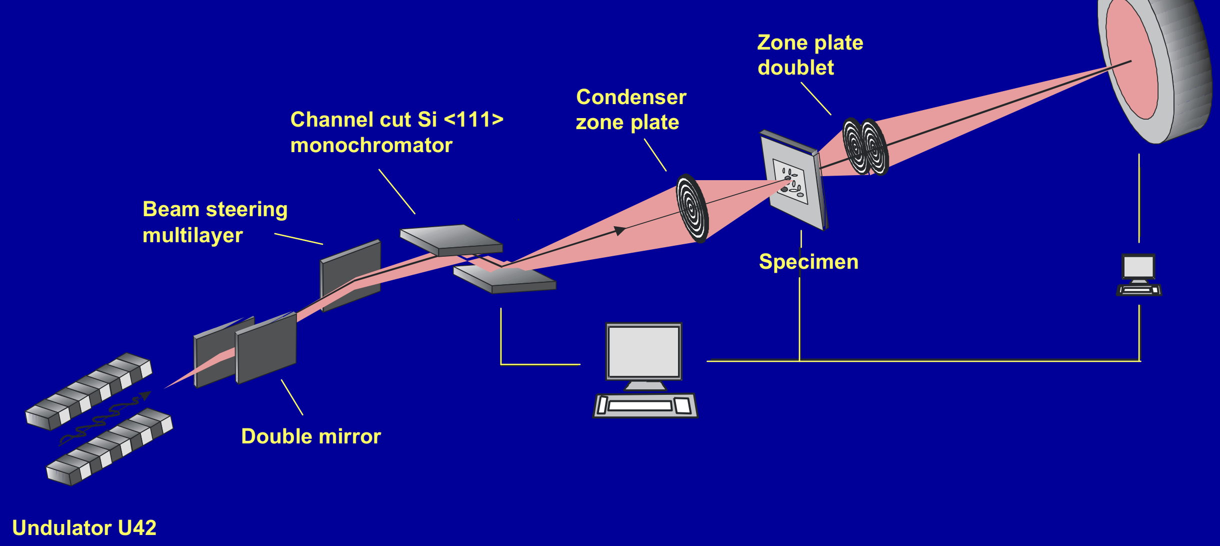

DIC with the scanning X-ray microscope: Optical setup

Scanning X-ray microscope at ID21 beamline, ESRF

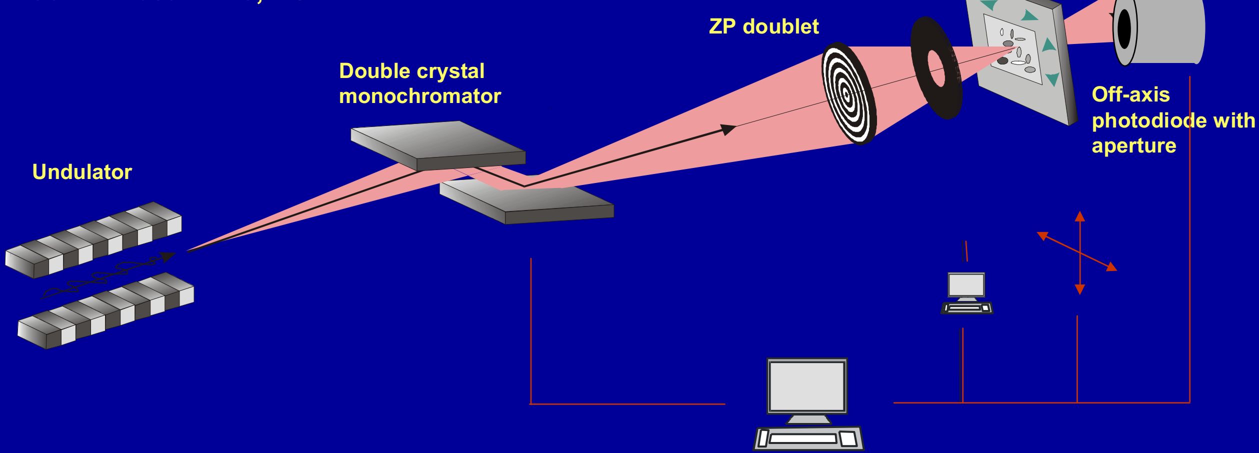

DIC with a scanning microscope (4 keV) using a ZP doublet

Brightfield

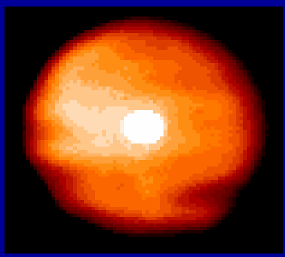

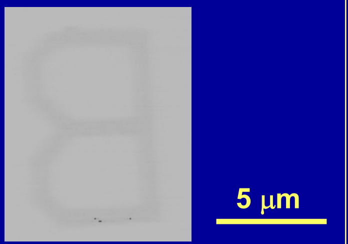

Contrast: 1.5 %

DIC

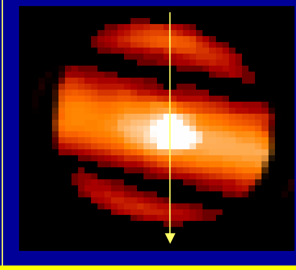

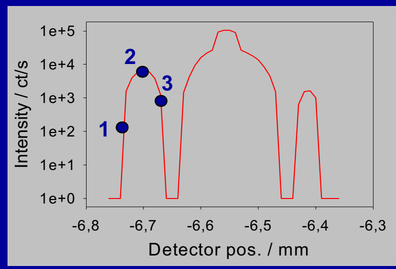

Raster scan of aperture detector across the first order diffracted light

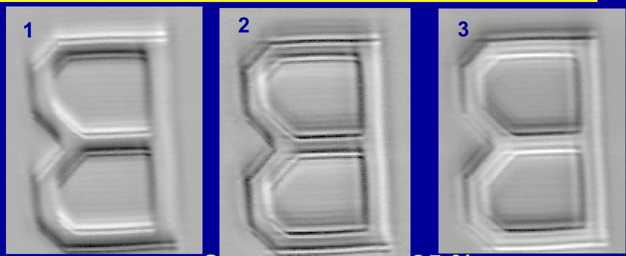

Contrast: up to 25 %

B. Kaulich, T. Wilhein, E. Di Fabrizio, F. Romanato, S. Cabrini, B. Fayard, J. Susini (Feb 2000)
B. Kaulich, B. Fayard, U. Neuhaeusler, M. Salome, J. Susini (March 2000)

Scalar versus Vectorial diffraction based models

Scalar based models

- ray traycing, spherical wave propagation + superposition
- phase retrieval iterative algorithms (PRIA)
- global optimization methods: genetic algorithms, simulated annealing

Vectorial based models

- Finite element method (FEM)
- Boundary element method (BEM)
- Method of moments (MOM)
- Finite-difference method (FDM)
- Finite-difference time-domain (FDTD)

Propagation operators for scalar approximation

1 Fraunhofer (far field); propagation operator: Fourier transform

$$z > \pi D^2 / 4\lambda$$

2 Fresnel (near field); propagation operator: Fresnel transform

$$\sqrt[3]{\pi D^4 / 64\lambda} \leq z \leq \pi D^2 / 4\lambda$$

3 very near field; propagation operator: the Fresnel-Kirchoff integral

$$\lambda << z < \sqrt[3]{\pi D^4 / 64\lambda}$$

High resolution tests

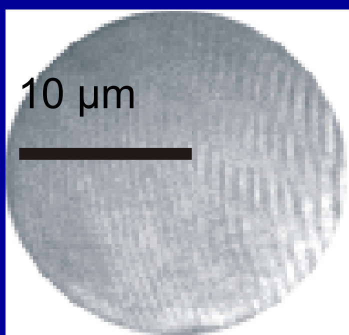

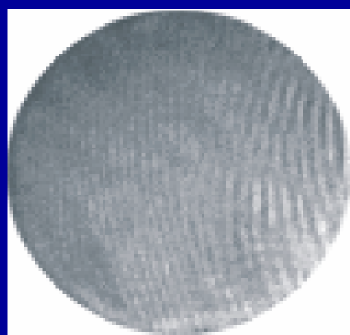

Objective lens: 2 confocal spots DOE

Sample: beamshaping DOE made by PMMA

Obs: the ultimate spatial resolution can be estimated being about 150 nm

Topography of biological samples @ 4 keV
Measured with 2 coaxial spot DOE (June 2001)

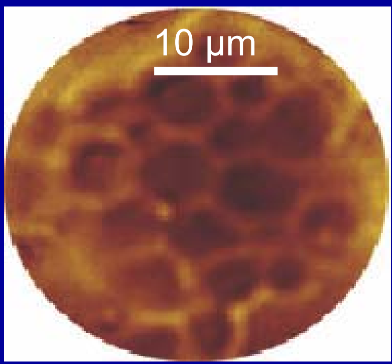

array of yeast cells

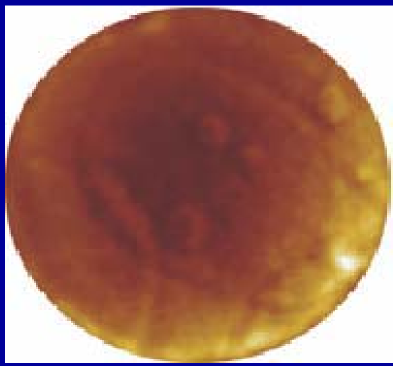

frog blood cells

Iris flower fibers

Simulation and measurements
for multi-spot ZP

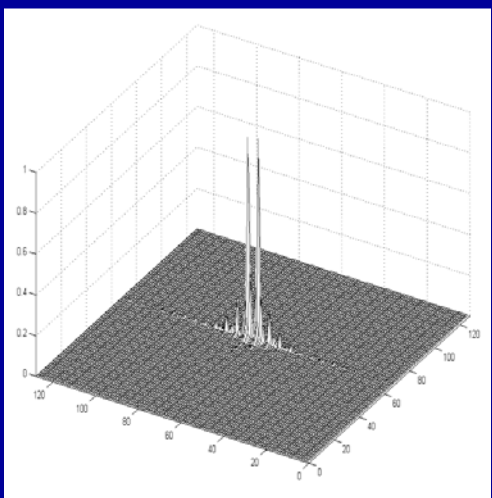

Simulation of 2-spot zone DOE in / out focal plane

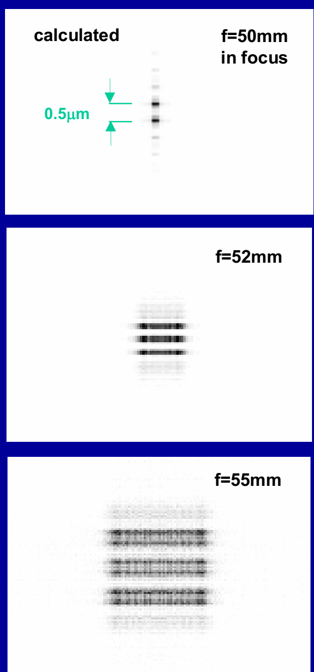

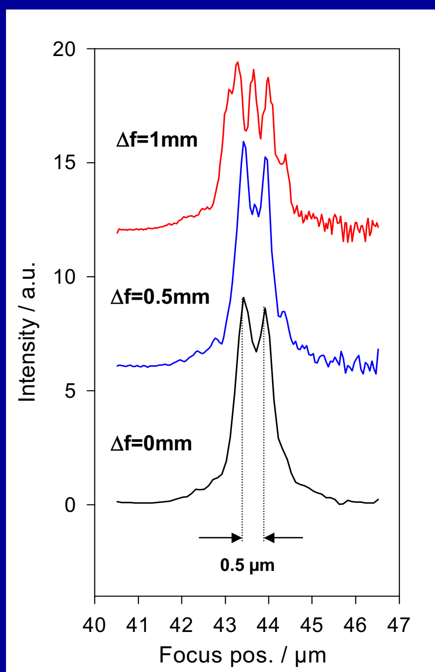

Comp. Simulations by: E. Di Fabrizio et.al (Lilit)
Measurements by: B. Kaulich, T. Wilhein, S. Cabrini, A. Barinov, J. Susini (Feb 2001)

Sum of oscillators

$$R = A[\cos \omega t + \cos(\omega t + \phi) + \cos(\omega t + 2\phi) + \cdots + \cos(\omega t + (n-1)\phi)], \quad (30.1)$$

$$A_R = A \frac{\sin n\phi/2}{\sin \phi/2}.$$

$$I = I_0 \frac{\sin^2 n\phi/2}{\sin^2 \phi/2}.$$

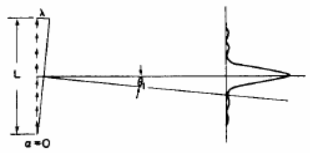

Fig. 30–5. The intensity pattern of a continuous line of oscillators has a single strong maximum and many weak "side lobes."

$$I = 4I_m \sin^2 \tfrac{1}{2}\Phi/\Phi^2.$$

are no higher-order maxima. If the scatterers are all in phase, we get a maximum in the direction $\theta_{out} = 0$, and a minimum when the distance Δ is equal to λ, just as for finite d and n. So we can even analyze a *continuous* distribution of scatterers or oscillators, by using integrals instead of summing.